BTO 2016.071 | August 2016

BTO report

PROBE-3: A succession model for ecosystem services

KWR Watercycle Research Institute

BTO

PROBE-3: A succession model for ecosystem services

BTO 2016.071 | August 2016

Project number
400554-115

Project manager
Edu Dorland

Client
BTO - Thematisch onderzoek - Klimaatbestendige watersector

Quality Assurance
Edu Dorland

Authors
Yuki Fujita, Ruud P. Bartholomeus, Jan-Philip M. Witte

Sent to
Themagroep Klimaatbestendige Watersector

Meer informatie
Yuki Fujita
T 030 60 69 707
E yuki.fujita@kwrwater.nl

KWR
PO Box 1072
3430 BB Nieuwegein
The Netherlands

KWR Watercycle Research Institute

BTO *Managementsamenvatting*

Nieuw successiemodel PROBE-3 geeft zicht op de invloed van weer en meststoffen op ecosysteemdiensten van grondwateronafhankelijke bodems

Auteurs dr. Yuki Fujita, dr ir. Ruud Bartholomeus en prof.dr.ir. Jan-Philip Witte

Het nieuwe successiemodel PROBE-3 is in staat te simuleren hoe drie ecosysteemdiensten (het scheppen van biodiversiteit, de reductie van stikstofuitspoeling en de aanvulling van het grondwater) in de loop der tijd veranderen onder invloed van het weer en de aanvoer van meststoffen. Het eendimensionale model produceert plausibele resultaten voor de nitraatuitspoeling onder bouwland en de duinen en voor de vegetatieontwikkeling op de noord- en zuidzijde van een droog duin. In tegenstelling tot eerdere (vlakdekkende) PROBE modellen, is PROBE-3 geschikt voor langetermijnprojecties waarbij rekening moet worden gehouden met veranderingen van de bodem onder invloed van zowel het plantendek als de weersgesteldheid en de aanvoer van nutriënten. Het dynamische successiemodel met terugkoppelingsmechanismen tussen bodem, water en vegetatie, is toepasbaar voor grondwateronafhankelijke bodems. Gedemonstreerd wordt hoe het model kan worden ingezet om de gevolgen te beoordelen van klimaatverandering en van atmosferische stikstofdepositie. Om de modelprestaties te verbeteren is ijking aan meer veldgegevens nodig. Daarna kan het worden gebruikt om snel rekenende relaties (metarelaties) te genereren ten behoeve van vlakdekkende PROBE-versies.

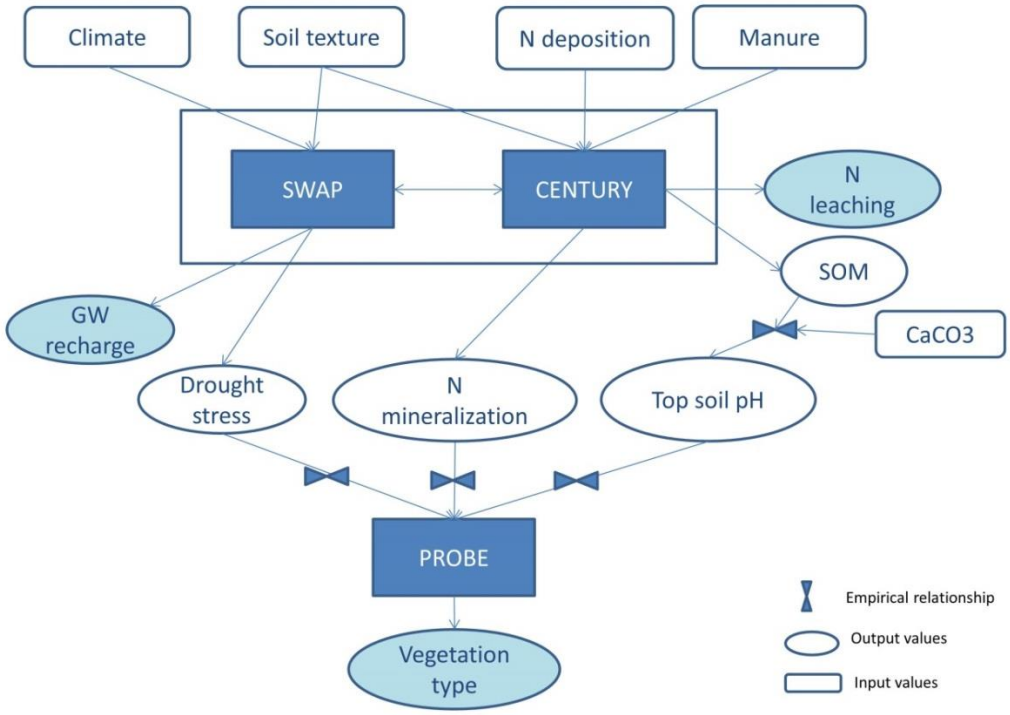

Dynamische koppeling van modellen voor bodemvocht (SWAP), organische stof en plantaardige productie (CENTURY), en vegetatiesamenstelling (vegetatiemodule PROBE)

Belang: voorspellen van ecosysteemdiensten

Naar verwachting heeft klimaatverandering grote gevolgen voor verschillende ecosysteemdiensten, zoals het scheppen van biodiversiteit, de reductie van stikstofuitspoeling en de aanvulling van het grondwater. Om de effecten van klimaatverandering en adaptatiemaatregelen te kunnen beoordelen is een klimaatrobuust procesmodel nodig.

Aanpak: koppelen van modellen

Het hier gepresenteerde model dat als eerste aan de gewenste vereisten voldoet – PROBE-3 – voorziet in een koppeling en dynamische simulatie van bodemvocht, organische stof en vegetatieontwikkeling. Het is een eendimensionaal model, dat we valideerden aan bodem- en vegetatiegegevens van verschillende successiestadia in een droog duingrasland. Met het model simuleerden we verschillende scenario's voor dit ecosysteem, variërend in helling, klimaat en atmosferische stikstofdepositie. Daarnaast zijn de gevolgen voor de nitraatuitspoeling van stikstofbemesting op een agrarisch grasland in Limburg (lössbodem) getest.

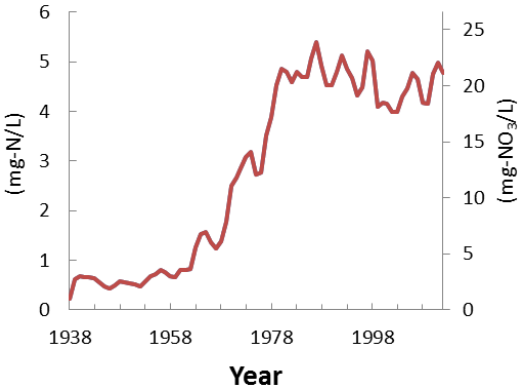

Gesimuleerd nitraatgehalte in het percolatiewater van een droog duin gedurende 75 jaar van vegetatieontwikkeling, beginnend met kaal zand

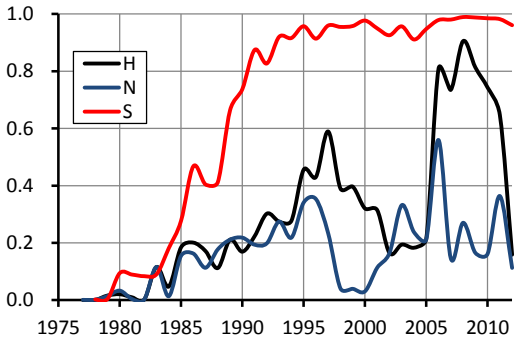

Met PROBE-3 gesimuleerde ontwikkeling gedurende 30 jaar van de Duin-Buntgras-associatie (14Aa02) op een horizontale bodem (H), en op de noord- (N) en de zuidhelling (S) van een duin.

Resultaten: ontwikkeling ecosysteemdiensten

De bodemontwikkeling, de vegetatiesamenstelling en de stikstofuitspoeling van het duingrasland worden door PROBE-3 bevredigend nagebootst. Volgens het model heeft klimaatverandering een geringe invloed op de opbouw van organische stof in de duinbodem. Gevolgen voor de ontwikkeling van de duinvegetatie zijn significant. Voor zowel het duingrasland als het landbouwperceel biedt het model een geloofwaardige nabootsing van het effect van stikstofdepositie en stikstofbemesting op de nitraatuitspoeling.

Implementatie: scenariostudies en metarelaties

Het nieuwe model PROBE-3 maakt het mogelijk om langetermijngevolgen van klimaatverandering, stikstofaanvoer en natuurlijke successie voor de ecosysteemdiensten na te bootsen. Meer veldgegevens zijn nodig ter verbetering van de modelparameters, maar ook voor een goede validatie van het model (bijvoorbeeld aan de waterfluxen en stikstofuitspoeling van lysimeters). Na verbetering en uitbreiding is het model ook toepasbaar voor het afleiden van metarelaties ten behoeve van vlakdekkende versies van PROBE.

Rapport

Dit onderzoek is beschreven in rapport *PROBE-3: A succession model for ecosystem services* (BTO 2016.071).

Meer informatie
Yuki Fujita
T 030 60 69 707
E yuki.fujita@kwrwater.nl

KWR
PO Box 1072
3430 BB Nieuwegein
The Netherlands

KWR Watercycle Research Institute

Contents

1	Introduction	2
2	Development of PROBE-3	4
2.1	Introduction	4
2.2	Modification of the CENTURY model	4
2.3	Modification of SWAP model	7
2.4	pH estimation	8
2.5	Coupling of SWAP, CENTURY and PROBE	9
3	Application of PROBE-3	13
3.1	Input data for model simulation	13
3.2	Model plausibility studies	14
3.3	Model scenario study	17
4	Results	19
4.1	Model plausibility study	19
4.2	Model scenario study	26
5	Discussion	34
5.1	Consequences of dynamic coupling of CENTURY and SWAP models	34
5.2	Plausibility and uncertainty of the models	35
5.3	Effects of slope and climate change	37
5.4	Effects of N input	37
6	Conclusions and recommendations	39

1 Introduction

Climate change is expected to have significant impacts on groundwater-independent ecosystems, since the moisture regime of these systems completely depends on precipitation and evapotranspiration demand (Witte *et al.*, 2012b). It is foreseen that not only temperature will rise, but also that more prolonged dry periods will alternate with more intensive rainfall events, both within and between years. This will change, among others, soil moisture dynamics (Easterling *et al.*, 2000; Weltzin *et al.*, 2003; Porporato *et al.*, 2004; Fay *et al.*, 2008; Knapp *et al.*, 2008). Soil moisture is the most important environmental filter of local terrestrial plant species composition, as it determines the availability of both oxygen and water to plant roots and, with that, indirectly other habitat factors that are essential for plant growth, such as soil acidity and nutrient availability (Easterling *et al.*, 2000; Weltzin *et al.*, 2003; Porporato *et al.*, 2004; Witte *et al.*, 2007b; Knapp *et al.*, 2008; Levine *et al.*, 2008; Bartholomeus *et al.*, 2011b).

In view of the projected change in climate and hydrology, it is questionable whether target ecosystems for nature preservation may still be attained under a future climate. This is important, since most of such targets are legally enforced, e.g. by the European Habitat Directive, by the Water Framework Directive, and by national legislations of several countries. For a timely response to climate change, as well as to avoid measures that may be ineffective, policy makers and spatial planners require information about the feasibility of nature targets under a future climate. It is inevitable that models are used for this purpose, because the empirical bases for climate change effects in the recent past, across transects that cover different climate zones, is too small. However, it is debatable whether current models are properly equipped for assessing climate change effects on nature targets.

In the last years KWR has been conducting two interconnected lines of eco-hydrological research: one on relationships between water-related habitat factors and vegetation patterns, and one on the effects of vegetation on evapotranspiration and groundwater recharge. An example of the first research line is de development of PROBE, which predicts vegetation types from habitat factors. The first model version has been developed for coastal dunes (Witte *et al.*, 2007a) and was applied in environmental impact assessment studies (De Haan & Doomen, 2006; De Haan & Witte, 2010). The knowledge underlying the PROBE model was further improved and deepened in multiple research projects (BTO, Climate Change Spatial planning, Knowledge for Climate, NOW Casimir, KWR innovation fund) with the final aim to create a more process-based and climate-versatile version. This second version of PROBE was launched in 2014 (Witte *et al.*, 2015a) and has been successfully applied in scenario studies on both regional and national scale (Van Ek *et al.*, 2014; Van der Knaap *et al.*, 2015; Witte *et al.*, 2015a; Van der Knaap *et al.*, submitted). In the second research line, we have conducted studies to understand the effect of vegetation on hydrology, especially on evapotranspiration and groundwater recharge. This line brought up new insights on: evapotranspiration characteristics of moss-dominated ecosystems (Voortman *et al.*, 2013a; Voortman *et al.*, 2015), the construction of weighable lysimeters (Voortman *et al.*, in prep; Voortman *et al.*, submitted), adaptation mechanisms of plants on drought and climate change (Witte *et al.*, 2006; Kruijt *et al.*, 2008; Bartholomeus *et al.*, 2011a; Witte *et al.*, 2012a), effects of slopes on evapotranspiration (Bartholomeus *et al.*, 2010), and the robustness of current evapotranspiration concepts (Bartholomeus *et al.*, 2013).

Climate change projections usually relate to a future of at least 20 years ahead, e.g. 2050 or 2100. Edaphic factors, such as organic matter content and pH, may change gradually but substantially within such a far climate horizon, especially in a changing climate. Our current models do, however, not account for these dynamic changes. With the knowledge progression presented in the previous paragraphs, it is now time to dynamically link both lines of research (i.e. effects of hydrology on vegetation and effects of vegetation on hydrology) in order to improve our understanding of the dynamic system behaviour of soil, water, and vegetation under changing climate. In this study, we will do so by developing a dynamic model, PROBE-3, to simulate development of ecosystems under changing climate. In succession of natural ecosystems a number of interactions between system elements play important roles. For example, nutrient availability for vegetation is influenced not only by soil organic matter content, but by soil moisture conditions as well. In turn, plants influence soil moisture conditions, soil physical characteristics, and leaching of nutrients to groundwater via uptake of nutrients, litter input to soil, and evapotranspiration.

The aim of this study is to develop a one-dimensional dynamic model of soil, hydrology, and vegetation, with which vegetation development, groundwater recharge and nitrate leaching to groundwater can be simulated for groundwater-independent soils. This output of PROBE-3 relates to two vital services of ecosystems to humankind: the provision of clean drinking water and biodiversity. Hence, PROBE-3 may be regarded as an ecosystem services model.

In this study we will first validate the model on the chronosequence data of natural dune grasslands in Luchterduinen, a nature reserve of drinking water company Waternet. Subsequently the model will be used to study effects of different scenarios (climate, nitrogen input, slope) on the development of soil and vegetation, groundwater recharge and N leaching in two model systems: natural dune ecosystems in Luchterduinen and a production grassland in the province of Zuid-Limburg.

2 Development of PROBE-3

2.1 Introduction

We developed a model which dynamically couples the hydrological model SWAP (Van Dam *et al.*, 2008), the soil and plant modules of CENTURY model (Parton *et al.*, 1987; Parton *et al.*, 1993), and the vegetation module of PROBE (Witte *et al.*, 2007b) (Figure 1). Prior to the coupling (§ 2.5), modifications were made in the CENTURY model (§ 2.2) and the SWAP model (§ 2.3). In addition, we made a repro-function of top soil pH based on empirical input data (§ 2.4).

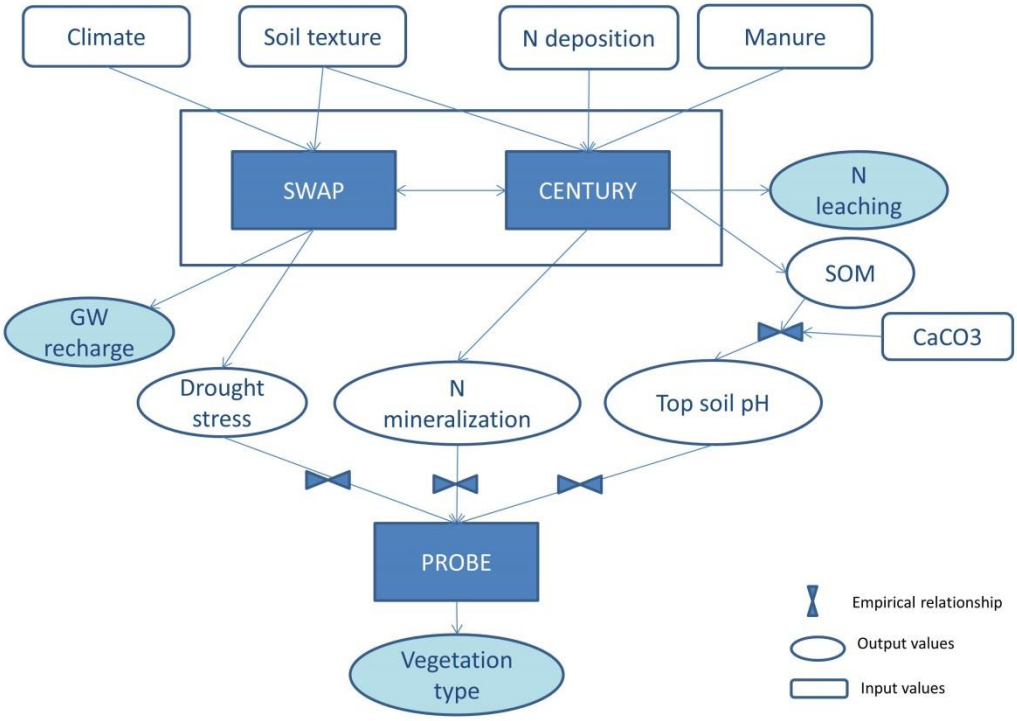

Figure 1. Coupling between CENTURY, SWAP and the vegetation module of PROBE. See text for further explanation.

2.2 Modification of the CENTURY model

We reconstructed CENTURY in the programming language Python, based on the equations specified in literature (Parton *et al.*, 1987; Parton *et al.*, 1993) and the source code of CENTURY version 4 (Metherell *et al.*, 1993). We used parameter values for 'C3 grasses' of version 4, unless specified otherwise. We defined three soil layers in the CENTURY model. Soil organic matter (SOM) accumulation occurs only in the top layer, whereas flows of mineral nitrogen are simulated in all three layers. We made a number of modifications in the model equations and parameter values as specified below, to better reflect moisture and temperature effects on SOM dynamics and plant production, as well as to make the model more applicable to the specific conditions of our target ecosystems.

Reduction of SOM decomposition due to suboptimal soil moisture conditions (i.e. too dry or too wet) was adapted in such a way that soil physical characteristics are explicitly incorporated (Fujita *et al.*, 2013b):

$$D = f_d f_w D_{pot} \quad [1.1]$$

Where D is the actual decomposition, f_d and f_w are reduction factors for wet and dry conditions respectively, and D_{pot} is the potential decomposition. Both reduction factors range between 0 (complete reduction) and 1 (no reduction).

The reduction factor f_d for dry conditions was formulated as:

$$f_d = \begin{cases} 1 & \psi_B \le \psi \\ 1 - \dfrac{\log(|\psi|) - \log(|\psi_B|)}{\log(|\psi_A|) - \log(|\psi_B|)} & \psi_A \le \psi < \psi_B \\ 0 & \psi < \psi_A \end{cases} \quad [1.2]$$

where ψ is the matric potential (kPa), ψ_B and ψ_A are the threshold values of ψ where drought starts and reaches the maximum, respectively. ψ_A and ψ_B were set to be -13.8MPa and -0.029 MPa (pF 5.13 and 2.46, respectively) according to Manzoni *et al.* (2011). The reduction factor f_w for wet conditions was formulated as:

$$f_w = \begin{cases} 1 & \varphi_{gas\_th} \le \varphi_{gas} \\ \dfrac{\varphi_{gas}}{\varphi_{gas\_th}} \cdot (1-m) + m & \varphi_{gas} < \varphi_{gas\_th} \end{cases} \quad [1.3]$$

where φ_{gas} is the soil gas content ($cm^3\ cm^{-3}$), φ_{gas_th} is the threshold of soil gas content where oxygen stress starts ($cm^3\ cm^{-3}$), and m is the level of anaerobic decomposition as a proportion to that of aerobic decomposition of a saturated soil. We set m as 0.24 to make it comparable to the level of decomposition under anaerobic conditions in CENTURY ver. 4. φ_{gas_th} was set as 0.2 $cm^3\ cm^{-3}$.

Moreover, based on De Wit (1958) the reduction term of plant growth due to suboptimal soil moisture conditions was adapted as follows:

$$M_P = \frac{T_{act}}{T_{pot}} \quad [1.4]$$

where M_p is the reduction term on plant growth, a fraction ranging from 0 (complete reduction) to 1 (no reduction), T_{act} is the actual transpiration rate (cm/day), T_{pot} is the potential transpiration rate (cm/day). T_{act} and T_{pot} are dynamically computed in SWAP on a daily basis.

The reduction term of plant growth due to temperature in CENTURY is formulated using a generalized Poisson distribution function:

$$T_P = \exp\left[\frac{p_3}{p_4}\left\{1-\left(\frac{p_2 - stemp}{p_2 - p_1}\right)^{p_4}\right\}\right]\cdot\left(\frac{p_2 - stemp}{p_2 - p_1}\right)^{p_3} \quad [1.5]$$

where p_1 and p_2 are the optimum and maximum temperature (°C) for plant production, respectively, p_3 is the parameter which shapes the left curve, p_4 is the parameter which shapes the right curve, and *stemp* is the soil temperature (°C). The parameter values for C3 grasses in CENTURY are: p_1 =15, p_2 =32, p_3 =1, p_4 =3.5. To restrict the plant production at low temperature, we change the value of p_4 from 3.5 to 5.

In CENTURY, plant death during the growing season is determined by soil moisture and shading. We replaced the moisture-dependent term of plant death, which is a function of volumetric water content in the root zone, with that of the SWAP model. The latter (i.e. the moisture-dependent plant death function of SWAP) uses the ratio between actual and potential transpiration of plants to compute leave senescence, allowing more realistic representation of drought effects on plant death. We combined the moisture-dependent shoot death and moisture-independent stem death of SWAP model to compute the death rate of the whole above-ground plant biomass:

$$S_s = w_{s1} + w_{s2}\left(1-\frac{T_{act}}{T_{pot}}\right) \quad [1.6]$$

where S_s is the moisture-dependent death rate of above-ground plant biomass (fraction/day), w_{s1} is the intercept value (fraction/day), w_{s2} is the maximum relative death rate due to moisture stress (fraction/day). For the intercept, we used the average death rate of young stem and old stem in SWAP divided by two (i.e. w_{s1}=0.005), with a simplified assumption that half of above-ground biomass is stems. Similarly, we set w_{s2} as the maximum relative death rate of leaves in SWAP divided by two (i.e. w_{s1}=0.015).

Further, we added an equation to set the maximum value in the relative plant growth rate, so that too rapid growth in the early stage of succession is avoided. We used the mean value of maximum relative growth rate of 105 UK plants measured on a weekly basis, 1.2 g/g/week [Dawson et al., 2011], which we converted to a daily value of 0.12 g/g/day, assuming exponential growth.

As in CENTURY, symbiotic N fixation is assumed to occur when soil mineral N is not sufficient to satisfy the plant N demand, having taken into account all the other factors which limit plant growth (e.g. temperature, moisture). Symbiotic N fixation can occur up to a maximum level of N fixed per C fixed, with a N:C ratio (*snfxmx*) specific to each plant type. Since CENTURY assumes monoculture crop systems, the value of *snfxmx* in CENTURY is either 0 gN/gC (for non-N-fixers) or 0.0375 gN/gC (for legume crops such as alfalfa). In natural ecosystems, however, symbiotic N-fixers (predominantly legume species) are ubiquitous and they typically occupy a few percent of the total cover. Thus, we introduce a new parameter, *nfxrat* (fraction between 0 and 1), to include the proportion of N fixers in plant production. We set the *nfxrat* value as the average value of symbiotic N fixers in two Dune ecosystems, Luchterduinen in the Netherlands and Newborough in UK, 0.03 (N=128, Fujita et al in prep).

We assumed that the asymbiotic N fixation (i.e. N fixation by free-living microorganisms) occurred at a constant rate. We used a the median value of temperate unfertilized grasslands (Reed *et al.*, 2011), 0.57 gN/m^2/yr. The fixed N is added to the ammonium pool of mineral N in the top soil.

The simulated size of passive pool of SOM was too small after decades of dune succession starting from a bare soil. This is because CENTURY is originally developed for very long (i.e. centuries) simulations of equilibrium ecosystems, whereas much shorter time scales (i.e. decades) are relevant for dune succession. Therefore, we modified the flow rate of active pool going into passive pool from 0.003 to 0.04, so that the percentage of passive pool after 75 years of simulation reaches approximately 20%, the same range as observed fraction of heavy C fraction in old dune grasslands (Kooijman *et al*., 2014).

Transport J of dissolved nitrogen in soil (g N/m^2/d) was calculated as the products of the water flows and the concentrations of dissolved N (N-NH4 + N-NO3) in the originating layer, assuming that dissolved nitrogen and water move at the same advective rate:

$$J = q \times C \qquad [1.7]$$

where q is the water flux (cm^3/m^2/d) and C is the concentration of mineral N (gN/cm^3). Diffusion and dispersion of dissolved nitrogen were not considered, since the advection is much larger than diffusion and dispersion in unsaturated zones. Daily N leaching rate was calculated as the sum of N transfer from the third soil layer into the deeper layer (gN/m^2/day). N leaching is simulated daily after plant uptake of nitrogen.

For production grasslands, we assumed that the 90% of above-ground biomass is harvested when it exceeds 300 g/m^2. Grazing by cows or rabbits was not included (although grazing is a possible extension of the model).

For production grasslands, we added an equation to regulate shoot:root ratio of newly-produced plant biomass, because otherwise roots grow unrealistically high in the frequently-harvested grasslands. We assumed that the root fraction in the newly-produced biomass, f_R, increases linearly with shoot:root ratio of the existing plant biomass as:

$$f_R = \min\left(s \cdot \frac{C_S}{C_R}, 0.5\right) \qquad [1.8]$$

where C_S and C_R are the amount of C in living above-ground and below ground biomass of the previous day (gC/m^2), respectively, s is the coefficient to determine the effect of the shoot:root ratio of the existing plant biomass on that of the newly-produced plant biomass. s was arbitrary set to be 1.

We also added an option of adding N via manure. It is common practice in agriculture in the Netherlands that organic manure is injected into the topsoil. However, for simplicity, we modelled that N is added in mineral forms (50% ammonium, 50% nitrate) to the top soil layer. To avoid unrealistic peaks in mineral N concentrations in soil, the annual amount of manure N was equally supplied from April to September by dividing it by the number of days in these months (183).

2.3 Modification of SWAP model

Vegetation on inclined surfaces with different aspects receives different amounts of precipitation (De Lima, 1990; Mentens *et al*., 2003; Schmidt & Mauersberger, 2009). To account for this, we transposed the precipitation measured on a horizontal surface at the weather station to the precipitation received by an inclined surface following the method of De Lima (1990).

We simulated the actual evapotranspiration with the SWAP model, using the potential evapotranspiration of a reference vegetation as input. We used the equation of Makkink (1957) to estimate the potential evapotranspiration of the reference vegetation. By definition, $ET_{Makkink}$ describes the evapotranspiration of a short grass vegetation not limited by a shortage of water. Input to Makkink's equation are daily global radiation and air temperature. We adjusted measured global radiation to the global radiation at an inclined surface, following the set of equations presented by Šúri and Hofierka (2004). Global radiation on inclined surfaces is described by three components: radiation that reaches the surface directly, radiation that has been scattered by atmospheric particles like clouds (diffuse radiation) and radiation reflected by the soil and that reaches the surface. Daily values of diffuse radiation were calculated with the method of Bindi *et al.* (1992), from measured global radiation on a horizontal surface at the nearest weather station.

For the small topographic features that we considered, climatic conditions like air temperature, wind speed and vapor pressure deficit may be assumed uniform across the landscape at the reference height (Bennie *et al.*, 2008). Therefore, the air temperature of inclined surfaces with a reference vegetation was assumed equal to that of a horizontal surface (Bennie *et al.*, 2008; Dyer, 2009).

2.4 pH estimation

Top soil pH_{KCl} was approximated using the empirical relationships of pH_{KCl}, $CaCO_3$ content, and soil organic matter content in chronosequence data of Luchterduinen (Aggenbach *et al.*, 2013) as:

$$pH_{KCl} = 5.112 + 0.328\ln(CaCO_3\% + 0.5) + (0.494d - 1.134)\ln(\max(0.045, SOM\%)) \quad [1.9]$$

where *CaCO3%* is the concentration of $CaCO_3$ (% d.w.), *SOM%* is the soil organic matter content (% d.w.), and *d* is the dummy variable for dune type (1 for lime-rich dune, 0 for lime-poor dune). *SOM%* was restricted to be greater than 0.045%, the minimum value in the empirical dataset.

$CaCO_3$ content can be approximated based on the dune age, according to Stuyfzand (2010):

$$CaCO3\% = 0.4CaCO3_0 \exp(-\alpha_1 t) + 0.6CaCO3_0 \exp(-\alpha_2 t) \quad [1.10]$$

where $CaCO3_0$ is the initial concentration of $CaCO_3$ (% d.w.), α_1 and α_2 are coefficients of decalcification speed ($year^{-1}$), and *t* is the age of the dune (year). We used empirically fitted values of the coefficients ($CaCO3_0$, α_1 and α_2) for top soils of 0-15cm depth in Luchterduinen (Aggenbach *et al.*, 2013): $CaCO3_0$=3.2%, α_1=0.085 $year^{-1}$ and α_2 =0.011 $year^{-1}$ for lime-poor dunes, and $CaCO3_0$=7.0%, α_1=0.041 $year^{-1}$ and α_2 = 0.009 $year^{-1}$ for lime-rich dunes (Figure 2).

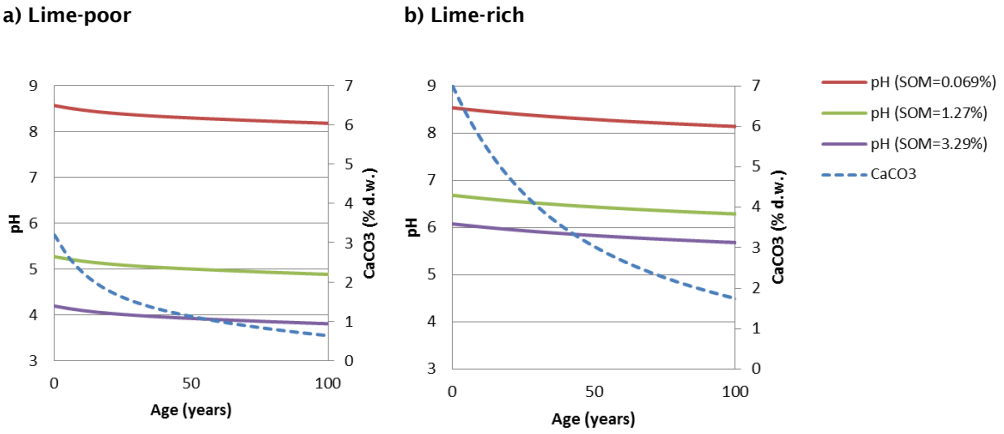

Figure 2. Repro-function of topsoil pH_{KCl} for lime-poor (a) and lime-rich (b) sites.

2.5 Coupling of SWAP, CENTURY and PROBE

2.5.1 Dynamic coupling of SWAP and CENTURY

Figure 3 shows how we coupled SWAP and CENTURY. At the end of every simulation year, soil organic matter content simulated by CENTURY was used to update pF parameters (i.e. θ_{sat}, n, α) of SWAP, using the repro-function derived from empirical data of Dutch soils (Wösten *et al.*, 2001). The repro-functions are:

$$\theta_{sat} = -35.7 - 0.1843 \cdot d - 0.03576 \cdot M_{50} + 0.0000261 \cdot M_{50}^{2} - 0.0564 \cdot p_{LEEM}^{-1} + 0.008 \cdot p_{HUMUS}^{-1} + 496.0 \cdot M_{50}^{-1} + 0.02244 \cdot \ln(p_{HUMUS}) + 7.56 \cdot \ln(M_{50}) \quad [1.11]$$

$$n = \exp\left\{\begin{matrix} -1.057 + 0.1003 \cdot p_{HUMUS} + 1.119 \cdot d + 0.000764 \cdot p_{LEEM}^{2} - \\ 0.1397 \cdot p_{HUMUS}^{-1} - 57.2 \cdot M_{50}^{-1} - 0.557 \cdot \ln(p_{HUMUS}) - 0.02997 \cdot d \cdot p_{LEEM} \end{matrix}\right\} + 1 \quad [1.12]$$

$$\alpha = \exp\left\{13.488 - 5.91 \cdot d + 0.003248 \cdot M_{50} - 11.89 \cdot d^{-1} - 2.121 \cdot p_{LEEM}^{-1} + 1.014 \cdot \ln(p_{LEEM})\right\} \quad [1.13]$$

where d is the soil bulk density (g/cm³), M_{50} is the median value of sand grain size (µm), p_{LEEM} is the percentage of clay plus silt in the soil, and p_{HUMUS} is the fraction of organic matter in the soil.

For the simulation of water loss by evapotranspiration we distinguished between 'vascular plants' and 'bare sand, mosses and lichens'. The latter group was defined on the basis of Voortman *et al.* (2013a) and Voortman *et al.* (2015), who found comparable evapotranspiration rates of mosses, lichens and bare sand. Hence, for simplicity, this group was simulated in SWAP as 'bare sand'. The modified reference evapotranspiration ($ET_{Makkink}$) described in § 2.3 was used as the potential evapotranspiration of vascular plants. Total evapotranspiration was simulated as a cover-weighted average of both groups. Plant biomass at the peak season simulated by CENTURY was used to update plant cover of the SWAP model. Here the following empirical relationship between plant biomass in summer and vascular plant cover of Dutch coastal dunes (N=62) (Aggenbach *et al.*, 2013; Fujita & Aggenbach, 2015) was used:

$$Cov_{herb} = 100 \frac{K \times P_0 \exp(r \times Bio)}{K + P_0 (\exp(r \times Bio) - 1)} \quad [1.14]$$

where cov_{herv} is the cover of vascular plants (%), *Bio* is the above-ground plant biomass in dry weight (g /m^2) at the peak season, *K*, P_0, *r* are the fitted parameter values found by non-linear regression (*K*=0.6165, P_0=0.0410, *r*=0.0520).

After the update of pF parameters and plant cover, SWAP was run for the next year. The following daily values of SWAP outputs were transferred into the CENTURY model as input: volumetric water content θ of each soil layer (cm^3/cm^3), soil water flows between soil layers (cm/day), soil temperature (˚C, average within the top soil layer), and potential and actual transpiration rate (T_p and T_a; cm/day).

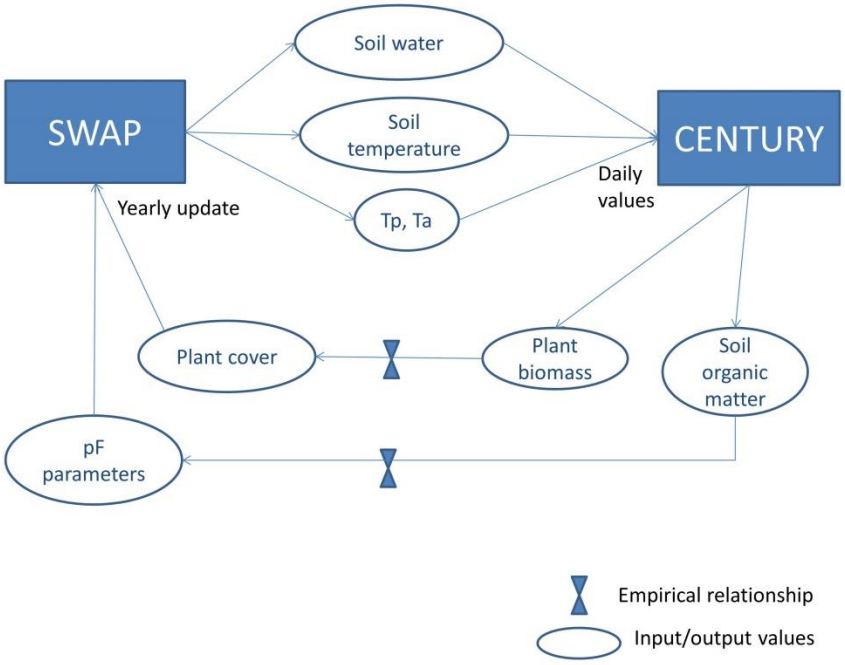

Figure 3. Coupling of SWAP and CENTURY model.

2.5.2 Coupling of SWAP-CENTURY to PROBE

At the end of each simulation year, potential drought and oxygen stress as defined by Bartholomeus *et al.* (2011b), N mineralization rate, and top soil pH_{KCl} was computed from the coupled SWAP-CENTURY model and the repro-function of pH. Based on this output, the vegetation module of PROBE predicted for each year an assemblage of vegetation types (Figure 1).

The vegetation module of PROBE describes the Baysian occurrence probabilities of vegetation types as a function of plot-mean indicator values for moisture (*mF*), nutrients (*mN*) and acidity (*mR*) (Witte *et al.*, 2007b). Drought stress and oxygen stress were converted to *mF* using the empirical relationship for the PROBE model developed for Dunea (Witte *et al.*, 2015b). This equation is meant for a large gradient in water regime, while our study focusses on a very narrow range of dry and nutrient poor sandy soils. To compensate for the bias created by this difference, we increased Eq. 3.3 in Witte *et al.* (2015b) with 5%. Note this 5% is a rough estimate based on expert judgement, not based on research. This correction resulted in the following relationship:

$$mF = 1.05 \cdot (3.24 - 25.303 \cdot RS + 10.6 \cdot TS + 1116 \cdot RS \cdot TS) \quad [1.15]$$

where *mF* is the plot-average indicator value for moisture, *RS* is the oxygen stress (kg O_2/m^2/10-day), and *TS* is the drought stress (kg H_2O/m^2/10-day).

The original PROBE model uses P mineralization rates as a proxy of nutrient availability to predict nutrient indicator values, whereas CENTURY simulates N mineralization rates only. Therefore, we made a new repro-function of N mineralization rate and *mN* based on empirical data of 136 plots in natural ecosystems in the Netherlands and Belgium (Fujita *et al.*, 2013a):

$$mN = \frac{1}{1+\exp\left(-b_0 - b_1 \cdot \log_{10}(Nmin+10)\right)} + b_2 + b_3 \cdot pH_{KCl} \qquad [1.16]$$

where *mN* is the plot-average indicator value for nutrients, *Nmin* is the annual N mineralization rate (mgN/kg soil/year), pH_{KCl} is the top soil pH-KCl, b_0, b_1, b_2, and b_3 are the fitted value of the regression model (R^2_{adj}=0.35, N=136); b_0 = -6.74648, b_1 =3.02408, b_2=0.49560, b_3=0.13787.

For the same reason for *mF*, we decreased existing equations for *mN* with a rough estimate of 10%. Thus, Eq. [1.16] becomes:

$$mN = 0.9 \cdot \left(\frac{1}{1+\exp\left(-b_0 - b_1 \cdot \log_{10}(Nmin+10)\right)} + b_2 + b_3 \cdot pH_{KCl} \right) \qquad [1.17]$$

Similarly, for the relationship between topsoil pH and *mR*, we decreased the relationship of Cirkel et al. (2014) with 5%:

$$mR = 0.95 \cdot \left(1.2604 \cdot \ln\left(pH_{KCl}\right) + 0.3361\right) \qquad [1.18]$$

where *mR* is the plot-average indicator value for acidity, pH_{KCL} is the pH_{KCl} in the top soil.

Since vegetation types do not instantaneously respond to the weather conditions of a certain year, we computed moving averages. Arbitrarily we took a time-frame of 4 years (except for the 1st, 2nd and 3rd year, for which the frame was 1, 2 and 3 years, respectively).

2.5.3 Construction of the vegetation module in PROBE

To construct the vegetation module in PROBE, we selected vegetation types that are considered as representatives of dune succession starting from a bare dune soil. We considered plant communities only at the association level.

Based on literature (DVN, Database Vegetation of the Netherlands), we selected six phyto-sociological associations (Table 1). Using the indicator values calculated section in §2.5.2, PROBE computes the occurrence probability *P* of each vegetation type. To this end PROBE utilizes probability density functions (pdfs) describing the Bayesian occurrence probability of vegetation types in dependency of plant traits or indicator values (Witte *et al.*, 2007b). Bayes' theorem meets the second Kolmogorov axiom, which means that the sum of *P* for each grid cell is always 100%. Gaussian Mixture Models were used to generate pdfs and are applicable to any vegetation classification system, as long as a large database of vegetation plots (relevés) is available. These pdfs are non-parametric, i.e. they do not assume a priori any

particular distribution of data points in the 3-D space. To acquire reliable pdfs, a minimum of 25 relevés per association was set as a minimum.

We used a national database (DVN, Database Vegetation of the Netherlands) to calculate the density functions. This database contains 35,000 relevés taken all over country in the period 1928-1988. DVN had been used for the standard work of vegetation types in the Netherlands (Schaminée *et al.*, 1995; Schaminée *et al.*, 1996; Schaminée *et al.*, 1998; Stortelder *et al.*, 1999). On the basis of their species composition, relevés of DVN were classified into associations. Additionally, indicator values *mF*, *mN*, and *mR* were computed for each relevé based on their species composition. Thus, the position of each classified relevé was obtained in a three dimensional space of indicator values. Combining all relevés from a vegetation type thus allows fitting the pdfs of vegetation types as a function of indicator values (Witte *et al.*, 2007b).

A randomly chosen half of the vegetation database DVN was used to calibrate pdfs, while the other half facilitated validation of the classification. In the validation, indicators values were used to predict, per relevé, the Bayesian occurrence probability P of the associations. Then each relevé was classified to the association for which the highest P was computed. Finally, we constructed a confusion matrix (Table 2). Each element of the matrix is indexed by the combination of 'observed' association (rows: classified on the basis of species composition) and 'predicted' association (columns: classified on the basis of indicator values) the number of relevés. Ideally, one hopes for a confusion matrix that consists of only diagonal elements, i.e. elements for which the 'predicted' association is exactly the same as the 'observed' association. All associations were classified reasonably well; The efficiency, i.e. the percentage of correctly classified relevés, is 82%.

Table 1. List of associations of plant communities considered in the PROBE model.

Code	Association
14AA02	*Violo-Corynephoretum*
14BB02	*Festuco-Galietum veri*
14CA01	*Phleo-Tortuletum ruraliformis*
14CB01	*Taraxaco-Galietum veri*
20AB01	*Carici arenariae-Empetretum*
20AB02	*Polypodio-Empetretum*

Table 2. Confusion matrix of the modelled vegetation types. # = number of plots used to create a GMD model, % percentage correctly classified plots.

Observed	Predicted						#	%
	14AA02	14BB02	14CA01	14CB01	20AB01	20AB02		
14AA02	174	10	9	1	1	8	203	86
14BB02	15	79	2	10		9	115	69
14CA01	6	5	188	13			212	89
14CB01	6	18	10	202		3	239	85
20AB01					15	6	21	71
20AB02	5	3		2	8	43	61	70
#	206	115	209	228	24	69		
%	84	69	90	89	63	62		

3 Application of PROBE-3

3.1 Input data for model simulation

We conducted model simulations for two sites; lime-rich and lime-poor dry dune grassland ecosystems on sandy soils in Luchterduinen, and agricultural lands (production grasslands) on loess soils in South Limburg. Both sites are groundwater-independent.

Historical Climate

For historical climate data of Luchterduinen, we used the meteorological data of the weather station De Bilt which has the longest historical climatic record in the Netherlands. Since the inland climate of De Bilt deviates from the coastal climate of Luchterduinen, the data of De Bilt was corrected for Valkenburg, the closest weather station to Luchterduinen, using the proportion between Bilt and Valkenburg weather stations in the recent year records. Daily meteorological data of De Bilt (precipitation, global radiation, air temperature, wind speed, wind direction, reference evapotranspiration of Makkink) was retrieved from KNMI.

Soil initial conditions (C, N, soil physical characteristics, root depth)

For Luchterduinen sites, when simulation started from bare soil, initial soil C and N content, N-NO3 and N-NH4 concentrations in soil water at any depth were all approximated as zero. Clay and silt content was assumed to be 0% and 5%, respectively. The median grain size of sand (M50) was assumed to be 200 µm. Initial soil physical characteristics (e.g. pF parameters) were approximated using the empirical relationships of Wösten *et al.* (2001) as specified in §2.5.1. In SWAP, soil water was simulated for 0 – 600 cm depth. In CENTURY, depth of the top layer (in which SOM accumulates), second layer, and third layer was set to be 0 – 20 cm, 20 - 310cm, and 310 – 595 cm depth, respectively. All plant roots were assumed to be distributed in the top soil layer.

For Limburg sites, we took typical value of production grasslands. Soil initial C content and N content were approximated from empirical data of 'brikgronden', the typical type of loess soil in South Limburg. We used the average values of top soil data of 5 sampling locations in South Limburg categorized as either 'BLd6-A' or 'BLb6-B' (Appendix 2 in Stiboka (1990)): soil organic matter 2.5%, Bulk density 1.42 kg/dm^3, clay content 14.8%, and silt content 77.6%. From these values, soil C per area (gC/m^2) was approximated as 3126 gC/m^2, using the empirical relationships between soil C per area, SOM in percentage, and bulk density in Luchterduinen. Since there was no data available for N content of the 'brikgronden', we used the global average C:N ratio of terrestrial grassland soils, 11.8:1 (Cleveland & Liptzin, 2007). Initial concentrations of mineral N in soil water was set based on the drinking water norm in the Netherlands (i.e. 11.3 mg N/L for nitrate, 0.045 mg N/L for ammonium). With the assumptions of soil pore space of 0.44 and 80% of water filled pore space, the initial concentrations for each layer were calculated as 3.97 * depth (m) for N-NO3 (gN/m^2) and 0.055 * depth (m) for N-NH4 (gN/m^2).

Plant initial conditions

For Luchterduinen sites, when simulation started from bare soil, we set the initial above-ground biomass, below-ground biomass, standing dead as zero.

Average annual production of production grassland under high manure levels in the Netherlands is approximately 1kg/m^2/year (Aarts *et al.*, 2005), which is approximately 500 gC/m^2/year. For Limburg sites, we set the initial above-ground biomass C (in January) as 10% of the annual production (50 gC/ m^2), standing dead biomass C as zero, and litter C as zero. Initial below-ground biomass C was set as the half of the annual above-ground C production (250 gC/m^2). C:N ratio of plants was assumed to be 16.4 (average values of production grassland (Aarts *et al.*, 2005)) for the above-ground biomass, and 52.5 for below-ground biomass (mean value of C:N ratio for CENTURY). Soil cover by vegetation was assumed to be 70%.

Atmospheric N deposition

We used the annual national average values of atmospheric N deposition (as NHx and NOy, both dry and wet, mol/ha/year) in the Netherlands. Historical average values from 1900 to 1980 was taken from Noordijk (2007), and the average values from 1981 to 2012 was retrieved from CBS *et al.* (2015). For Luchterduinen simulation, the national average of N deposition level was corrected for the local level N deposition level of Luchterduinen for the period after 1946, by using the proportion of the local over the national average in 2014 (Velders *et al.*, 2015), i.e. 84%.

3.2 Model plausibility studies

3.2.1 Field observation data for soil C and N accumulation

In 2012 Aggenbach *et al.* (2013) measured soil C and N accumulation in chronosequence of dune grasslands in Luchterduinen. The field measurement took place in the grasslands which fall into one of the following five age categories: 6-11 years old, 11-22 years old, 22-33 years old, 33-44 years old, and >74 years old. For each age category, the model was run for the corresponding period of time (i.e. 8 years from 2005 to 2012, 16 years from 1997 to 2012, 27 years from 1986 to 2012, 38 years from 1975 to 2012, and 75 years from 1938 to 2012).

The simulated soil C accumulation rate, soil N accumulation rate, and above-ground vascular plant biomass at the peak season were compared to the observed values.

3.2.2 Filed observation data for vegetation type

For validation of vegetation types, we selected 30 plots from the chronosequence of dry dunes in Luchterduinen (Aggenbach *et al.*, 2013): five plots for each of three age categories (6-11 years old, 33-44 years old, and >74 years old) for both lime-rich and lime-poor dunes. The plant relevee data was classified into associations using the program Turboveg and Expert judgement of Camiel Aggenbach (KWR).

3.2.3 Field observation data for N leaching

Although we do not have observation data of N leaching from the above-mentioned plots, several literatures provides information about the expected range of N leaching rates in the target ecosystems. We used the following data to qualitatively validate our model outputs of N leaching.

N leaching under different vegetation types

Nitrate concentration data in shallow groundwater in AWD (Stuyfzand, 1991) was used for validation of N leaching rates. In multiple years between 1979 and 1986, samples were taken from 0.5 to 2 m depth in 18 locations with contrasting vegetation types. Of 18 locations, we

used the data of 6 locations; 3 locations under moss vegetation (“mossen-1”, “mossen-2”, “mossen-3”) and 3 locations under grass vegetation (“grassen-1”, “grassen-2”, “grassen-3”). The simulated N leaching rates in sandy soil was qualitatively compared with the average nitrate concentrations in each location, as shown in Figure 5.1 of Stuyfzand (1991) (Figure 4).

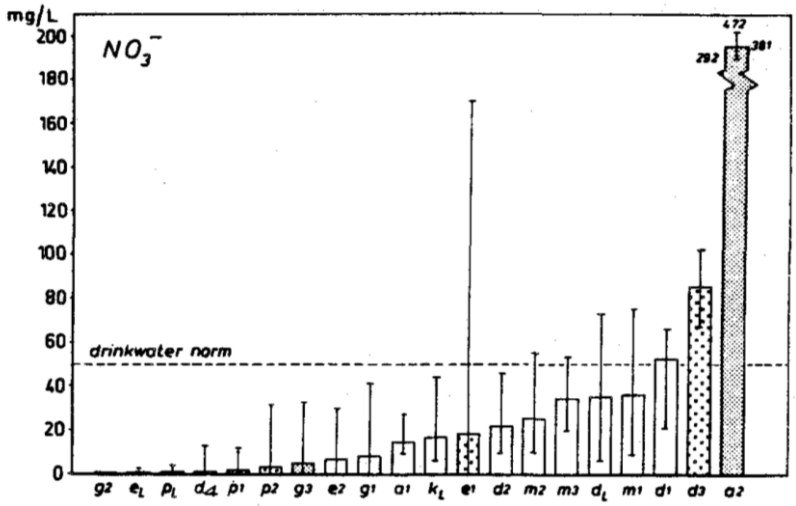

Figure 4. Average NO3- concentrations (mg/L) in the shallow groundwater of 16 sampling points in Luchterduinen and 4 lysimeters in Castricum. Minimum and maximum values are shown with bars. Vegetation types are: a: ferns, d: Hippophae rhamnoides, e: oaks, g: grasses, m: mosses, p: pines. Figure 5.1 of Stuyfzand (1991)

Temporal fluctuation of N leaching

Temporal fluctuation of N leaching rates in relation to atmospheric N deposition was qualitatively compared with the long-term observation data of nitrate concentrations in rain water (Figure 5) and in lysimeter drainage water (Figure 6) in Castricum.

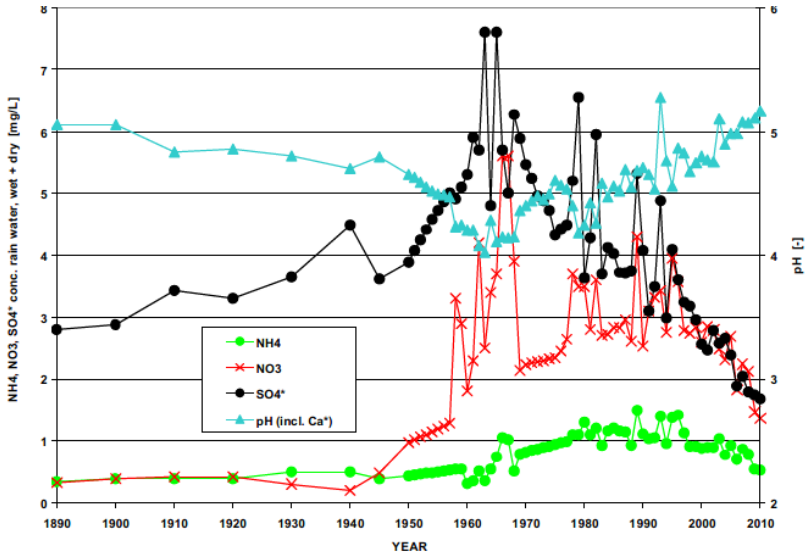

Figure 5. Concentration of, among others, NO3and NH4 (mg/L) in rainwater along the Nehterlands coast such as Castricum. Figure 3.8 of Stuyfzand and Rambags (2011).

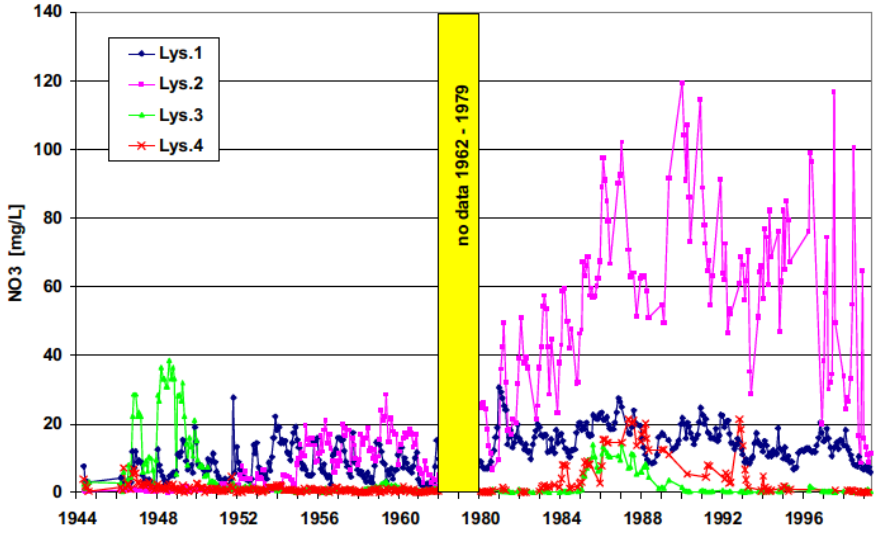

Figure 6. NO3 concentrations in drainage water of four lysimeters in Castricum from May 1944 to May 1999. The vegetation type of lysimeters are Lys 1: bare soil, Lys.2: dune grassland (which was invaded by Hippophae rhamnoides in the late stages), Lys.3: Oak forest, and Lys.4: Pine forest. Figure 3.16 of Stuyfzand and Rambags (2011).

N leaching under agricultural soils

We referred to nitrate concentration in ground water under agricultural companies on loess soils measured by PBL between 2002 and 2010 (Willems & van Schijndel, 2012). Number of observation points was 14 – 44 (varied among year). Average nitrate concentration was approximately 82 mg-NO3/L (which is equivalent to ca. 19 mg-N/L) (Figure 7). Nitrate concentration was in general higher under crop lands (‘akkerbouw’, on average 115 mg-NO3/L) than under pasture (‘melkvee’, on average 54 mg-NO3/L).

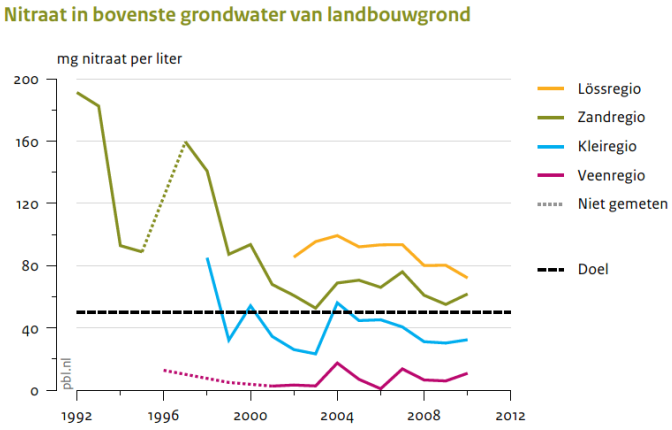

Figure 7. Nitrate concentration in top groundwater under agricultural soils. Figure 3.2 of Willems and van Schijndel (2012)

3.3 Model scenario study

For Luchterduinen, scenario study was conducted with different assumptions of slope, future climate, and N input level. For Limburg, scenarios with different levels of manure were tested. See Table 3 for overview of the scenarios tested.

As slope scenario, we simulated flat surface, south-facing slope, and north-facing slope for 38-year-old dune grasslands in Luchterduinen, with actual climate and actual N deposition level from 1975 to 2012. The tested slopes are: south facing slope (orientation 180 degrees, inclination 30 degrees), north facing slope (orientation 0 degrees, inclination 30 degrees) and flat (inclination 0 degrees).

As future climate scenario, we used the projected values of precipitation, evapotranspiration, and temperature for the 30 years, computed from the past meteorological data of 1981 – 2010 of weather station Valkenburg. The selected climate scenarios for model simulation are 'H' (reference) and 'W+' (global temperature increase is high and change in air circulation pattern is high). We used two starting conditions: bare sand and old grassland. The initial conditions of soil and vegetation of the old grassland were taken from the prior simulation of grasslands for 75 years in Luchterduinen.

As N deposition scenario, we assumed two levels of N deposition: high N deposition (i.e. the level of 2013 in the Netherlands) and low N deposition (i.e. the level of 1900 in the Netherlands). The model was run for 30 years with actual climate data of 1981-2010 from weather station Valkenburg. We used two starting conditions: bare sand and old grassland.

As manure scenario, four levels of manure input were applied from no manure to high level of manure. For the high manure level, we used the maximum amount of N in manure allowed in the manure policy 2015-2017 for grasslands on loess soils, 320 kg/ha/year (retrieved from http://www.rvo.nl/sites/default/files/20150723%20Tabel%201%20Stikstofgebruiksnormen%202015-2017.pdf on 2015-08-20). The model was run for 30 years with actual N deposition rates of the Netherlands of 1981-2010, and with actual climate data of 1981-2010 from the weather station Maastricht.

Table 3. Overview of model validation study and model scenario studies.

area	Simulation year	Climate	N deposition	Initial condition	Slope	Manure
Validation						
Luchterduinen	**2005-2012**	actual*1	actual*2	bare	flat	none
	1997-2012	actual*1	actual*2	bare	flat	none
	1986-2012	actual*1	actual*2	bare	flat	none
	1975-2012	actual*1	actual*2	bare	flat	none
	1938-2012	actual*1	actual*2	bare	flat	none
Slope scenarios						

Luchterduinen	1975-2012	actual*1	actual*2	bare	**flat**	none
	1975-2012	actual*1	actual*2	bare	**South***3	none
	1975-2012	actual*1	actual*2	bare	**North***4	none
Climate scenarios						
Luchterduinen	1981-2010	**actual (H)***5	2013 level	**bare**	flat	none
	2036-2065	**W+**	2013 level	**bare**	flat	none
	1981-2010	**actual (H)** *5	2013 level	**grassland***6	flat	none
	2036-2065	**W+**	2013 level	**grassland***6	flat	none
N input scenarios						
Luchterduinen	1981-2010	actual*5	**2013 level**	**bare**	flat	none
	1981-2010	actual*5	**1900 level**	**bare**	flat	none
	1981-2010	actual*5	**2013 level**	**grassland***6	flat	none
	1981-2010	actual*5	**1900 level**	**grassland***6	flat	none
Manure scenarios						
Limburg	1981-2010	actual*7	actual*8	pasture	flat	**4 levels (from none to high***9**)**

*1: historical meteorological data of De Bilt weather station, corrected for Valkenburg weather station

*2: National average N deposition data, corrected for Luchterduin area

*3: inclination 30°, orientation 180°

*4: inclination 30°, orientation 0°

*5: actual meteorological data of Valkenburg weather station

*6: 75-years-old dune grassland, simulated for 1938-2012 with the historical data of climate and N deposition

*7: actual meteorological data of Maastricht weather station

*8: National average N deposition data

*9: 0, 160, 240, 320 kgN/ha/year (= 0, 16, 24, 32 gN/m^2/year)

4 Results

4.1 Model plausibility study

4.1.1 Succession of soil in Luchterduinen

Our model was able to simulate soil C and N accumulation rates of different succession ages well (Figure 8 a & b). The modelled values of soil C and N accumulation were in the same range as the observed values in 2012, except that the model underestimated soil N accumulation for young grasslands (i.e. 8 and 16 years old). The accumulation rates of soil C and soil N in the first decades were slower for 75-year simulations than the other simulations, reflecting much lower atmospheric N deposition rates before 1970's.

Our model overestimated plant biomass compared to the field observation (Figure 8c). This could be because the observed biomass was underestimated due to occasional presence of grazing animals (e.g. rabbits). Interannual fluctuation in plant biomass was caused by variations in climatic conditions, namely soil temperature and soil moisture.

Top soil pH in lime-rich and lime-poor dunes was simulated well by our reprofunctions (Figure 8d and Figure 8e).

a) Soil carbon

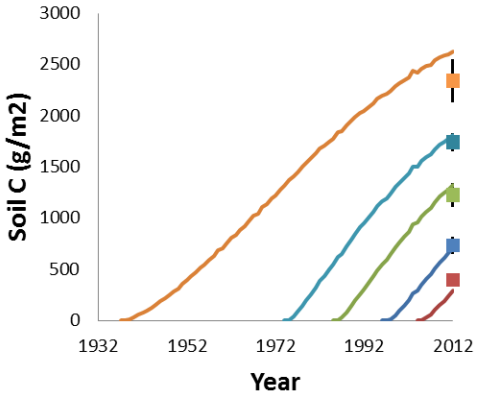

b) soil nitrogen

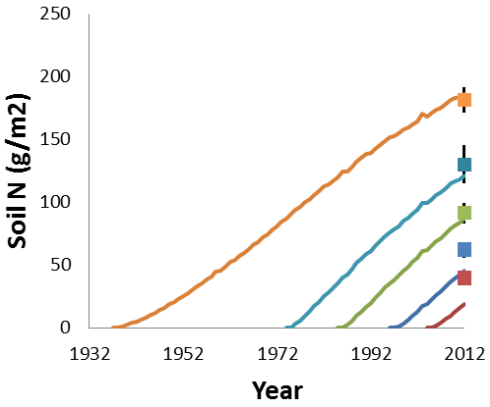

c) above-ground plant biomass

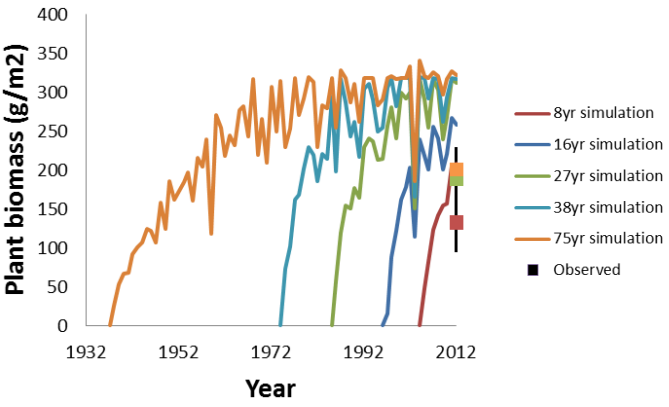

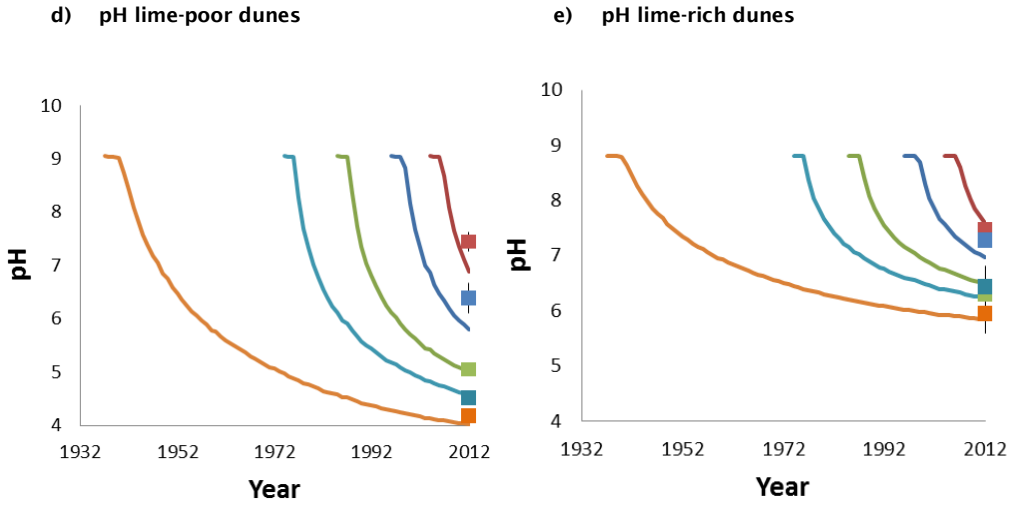

Figure 8. Simulated soil C (a), soil N (b),above-ground vascular plant biomass at peak season (c), top soil pH in lime-poor dunes (d) and lime-rich dunes (e) on a horizontal dune soil of Luchterduinen for the period of 8 years (2005-2012), 16 years (1997-2012), 27 years (1986-2012, 38 years (1975-2012), and 75 years (1938-2012). Squares show observed values in the field in 2012 (average and SE, lime-rich and lime-poor sites together for a), b), and c)) . Observed biomass values for 16-year and 38-year are missing.

4.1.2 Succession of vegetation in Luchterduinen

Before presenting the simulation results it should be noted that the graphs in this section have been made by averaging simulated indicator values over an arbitrarily chosen time frame of four years (Section 2.5.2). This means that the simulated response of the vegetation to soil succession and weather may be too strong for an association mainly consisting of geophytes, whereas a pioneer vegetation would show a quicker response than simulated. We will come back to this issue in Chapter 5.

In the course of 75-year dune succession, predicted vegetation associations changed dynamically (Figure 9).

Lime-poor sites (Figure 9 top) become dominated by 20AB02 *Polypodio-Empetretum* and 14AA02 *Violo-Corynephoretum*, especially at the expense of 14CA01 *Phleo-Tortuletum ruraliformis* (disappears in ca. one decennium), 14CB01 *Taraxaco-Galietum veri* (disappears in ca. four decennia) and 14BB02 *Festuco-Galietum veri* (takes the whole period of 75 years to fade away). The dominance of 14CA01 *Phleo-Tortuletum ruraliformis*, 14CB01 *Taraxaco-Galietum veri* and 14BB02 *Festuco-Galietum veri* in the first decades of the succession is caused by a high initial pH value, which declines to values lower than 6 after more than two decades (Figure 8d). 20AB01 *Carici arenariae-Empetretum* pops-up after about two decennia, after which it does not show a clear trend.

Lime-rich sites (Figure 9 bottom) become dominated by 14BB02 *Festuco-Galietum veri* in the course of succession. 14CA01 *Phleo-Tortuletum ruraliformis* again appears as a pioneer vegetation. 14CB01 *Taraxaco-Galietum veri* reaches its maximum after 15-35 years, after a gradual decline sets in.

For both lime-poor and lime-rich dunes, the extremely wet period (1965-1968) caused peaks of 14CB01 *Taraxaco-Galietum veri*, and the extremely dry period (1975-1977) caused peaks of 14AA02 *Violo-Corynephoretum* and in lime-rich dunes 14CA01 *Phleo-Tortuletum ruraliformis*.

Figure 10 (lime-poor) and Figure 11 (lime-rich) show the simulated succession of six vegetation types for different ages (i.e. different starting time of succession). Although the dunes with different ages experienced different weather conditions and N-deposition, the succession trajectories of each vegetation type were not clearly different among ages.

The predicted vegetation associations coincide roughly with the observed vegetation in the field (Table 4). 14AA02 *Violo-Corynephoretum* was observed only in lime-poor sites on different successional stages; in the model this association also primarily occur in lime-poor dunes on various successional stages. 14CA01 *Phleo-Tortuletum ruraliformis* was observed in the early successional stages (6-11 years) in both lime-rich and lime-poor dunes, and this pattern coincides with the model prediction. 14BB02 *Festuco-Galietum veri* was observed both in lime-rich and lime-poor dunes and mainly in old successional stages, whereas in the model it was more often predicted in old lime-rich dunes. 14CB01 *Taraxaco-Galietum veri* was in the field the predominant association in old lime-rich dunes, whereas in the model it was predicted to occur only marginally in old lime-rich dunes. Note that we only selected herbaceous vegetation to establish the plots. This is why the heath vegetation (20AB01 and 20AB01) does not appear in the field records, whereas they are the typical vegetation types occurring in the late successional stages of lime-poor dunes.

The predicted succession patterns are also largely in line with Schaminée and Jansen (1998), yet some deviations were identified. The main heath vegetation that is predicted in lime-poor dunes (20AB02 *Polypodio-Empetretum*) is actually representative for north slopes, while in flat lime-poor dunes the heath type 20AB01 *Carici arenariae-Empetretum* predominates. The latter type however is only marginally predicted by our model. In lime-rich dunes the presence of 14CB01 *Taraxaco-Galietum veri* is underestimated in favour of 14BB02 *Festuco-Galietum veri,* except during periods with several extremely wet years.

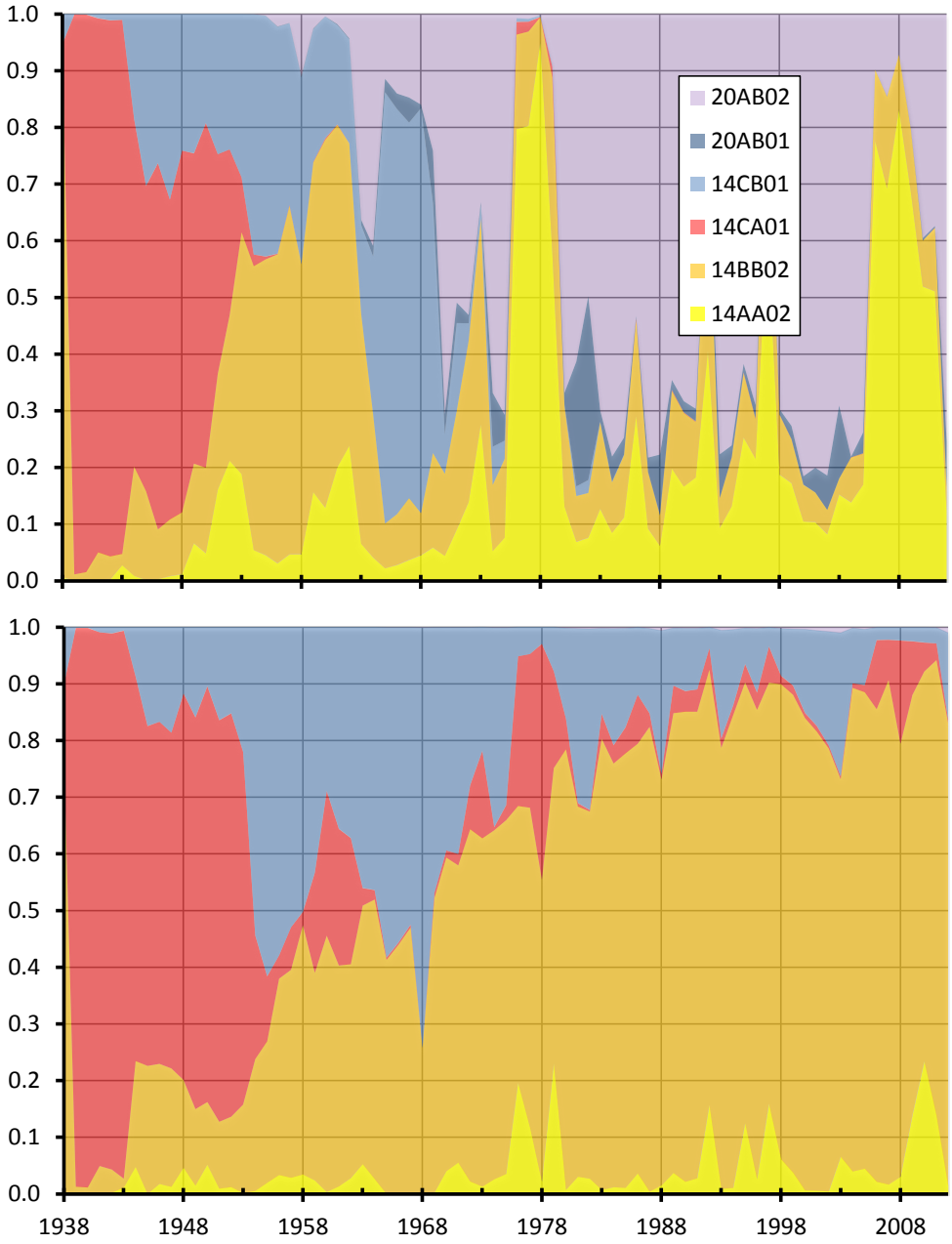

Figure 9. Simulated probability of occurrence of six vegetation associations for 75-year dune succession starting from a horizontal bare soil in lime-poor (top) and lime-rich (bottom) dune areas.

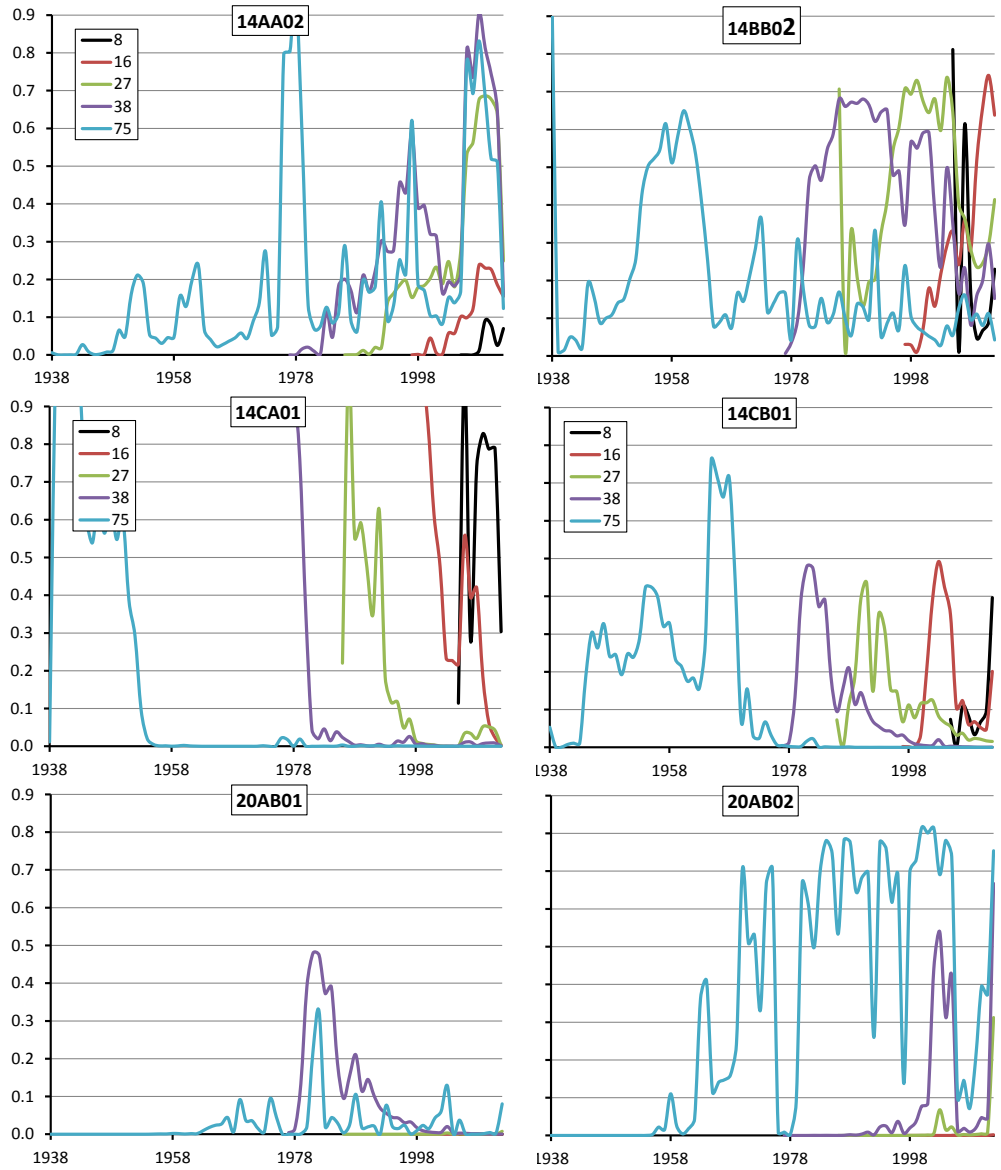

Figure 10. Simulated probability of occurrence of six vegetation associations for the period of 8 years (2005-2012), 16 years (1997-2012), 27 years (1986-2012, 38 years (1975-2012), and 75 years (1938-2012) on a lime-poor horizontal dune soil.

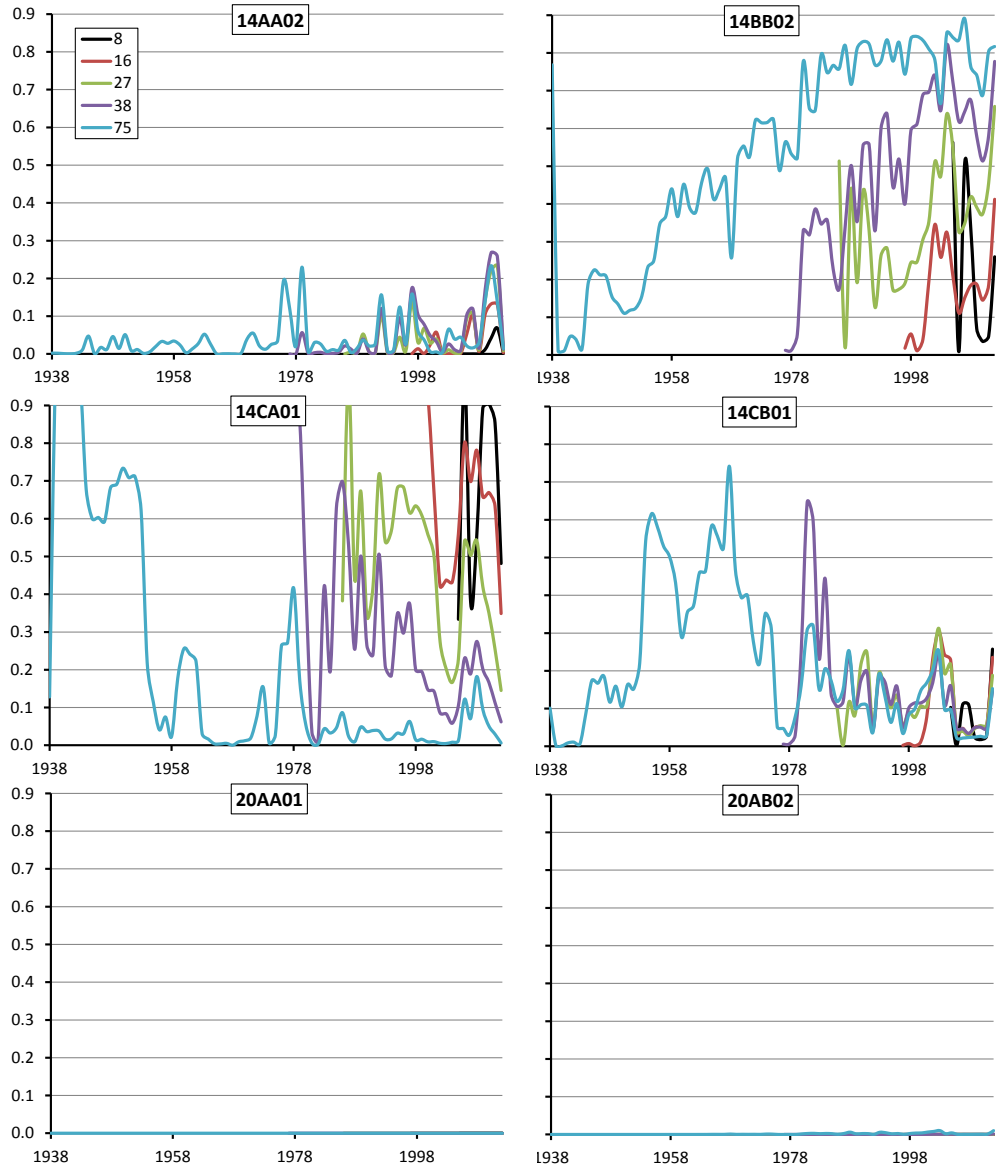

Figure 11. Simulated probability of occurrence of six vegetation associations for the period of 8 years (2005-2012), 16 years (1997-2012), 27 years (1986-2012, 38 years (1975-2012), and 75 years (1938-2012) on a lime-rich horizontal dune soil.

Table 4. Associations of different age classes on lime-poor and lime-rich dune grasslands, observed in Luchterduinen.

Plot Nr	Age	Lime richness	Association	Association name
20	6-11	poor	14AA02B	*Violo-Corynephoretum koelerietosum*
22	6-11	poor	14CA01A	*Phleo-Tortuletum typicum*
23	6-11	poor	14CA01A	*Phleo-Tortuletum typicum*
24	6-11	poor	14CA01A	*Phleo-Tortuletum typicum*
25	6-11	poor	14CA01A	*Phleo-Tortuletum typicum*
83	6-11	rich	14CA01A	*Phleo-Tortuletum typicum*
86	6-11	rich	14CA01A	*Phleo-Tortuletum typicum*
87	6-11	rich	14CA01A	*Phleo-Tortuletum typicum*
88	6-11	rich	14CA01A	*Phleo-Tortuletum typicum*
89	6-11	rich	14CA01A	*Phleo-Tortuletum typicum*
1	33-44	poor	14AA02B	*Violo-Corynephoretum koelerietosum*
2	33-44	poor	14AA02B	*Violo-Corynephoretum koelerietosum*
3	33-44	poor	14RG01	*RG Carex arenaria-[Koelerio-Corynephoretea]*
4	33-44	poor	14BB02A	*Festuco-Galietum typicum*
5	33-44	poor	14AA02B	*Violo-Corynephoretum koelerietosum*
71	33-44	rich	37RG03	*RG Hippophae rhamnoides-Calamagrostis epigejos-[Berberidion vulgaris/Polygalo-Koelerion]*
72	33-44	rich	37RG03	*RG Hippophae rhamnoides-Calamagrostis epigejos-[Berberidion vulgaris/Polygalo-Koelerion]*
73	33-44	rich	37RG03	*RG Hippophae rhamnoides-Calamagrostis epigejos-[Berberidion vulgaris/Polygalo-Koelerion]*
74	33-44	rich	37RG03	*RG Hippophae rhamnoides-Calamagrostis epigejos-[Berberidion vulgaris/Polygalo-Koelerion]*
76	33-44	rich	14RG09	*RG Calamagrostis epigejos-[Cladonio-Koelerietalia]*
37	>74	poor	14AA02B	*Violo-Corynephoretum koelerietosum*
38	>74	poor	14AA02B	*Violo-Corynephoretum koelerietosum*
39	>74	poor	14BB02A	*Festuco-Galietum typicum*
40	>74	poor	14RG03	*RG Dicranum scoparium-[Koelerio-Corynephoretea]*
41	>74	poor	14RG03	*RG Dicranum scoparium-[Koelerio-Corynephoretea]*
60	>74	rich	14CB01A	*Taraxaco-Galietum cladonietosum*
151	>74	rich	14BB02A	*Festuco-Galietum typicum*
154	>74	rich	14BB02A	*Festuco-Galietum typicum*
159	>74	rich	14CB01A	*Taraxaco-Galietum cladonietosum*
161	>74	rich	14CB01A	*Taraxaco-Galietum cladonietosum*

4.1.3 N leaching

As observed in Castricum lysimeters (see Figure 5 and Figure 6), simulated N leaching in our model synchronized more or less with the atmospheric N deposition (Figure 12). The magnitude of simulated N leaching in our model in the last decades (ca. 4-5 mg N/L, which is equivalent to nitrate concentrations of ca. 18-22 mg NO_3/L) is in the same range as the field observation: in Castricum the observed nitrate leaching in lysimeter under bare soil was ca. 10-30 mg NO_3/L (Figure 6), and in Luchterduinen the observed nitrate concentrations in shallow groundwater under grasses and mosses were 5-20 mg NO_3/L and 25-35 mg NO_3/L, respectively (Figure 4). Note that the modelled N leaching rates remained high in the last

decades despite of the decrease in atmospheric N deposition after 1990's. This implies that the effect of elevated N deposition on N leaching does not disappear immediately after N deposition is reduced, because of accumulated N in vegetation and soil.

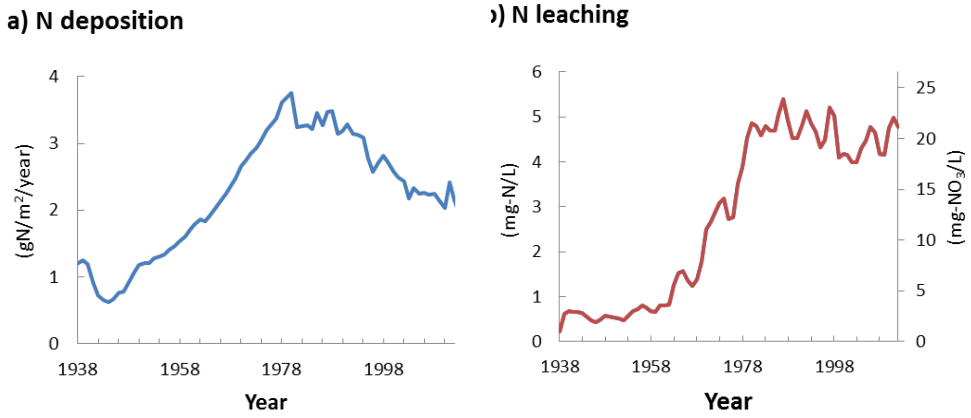

Figure 12. Historical atmospheric N deposition rate (NHx+NOy) (left) and simulated N leaching to groundwater (right) in Luchterduinen from 1938 to 2012. The historical N deposition rates were retrieved from Noordijk (2007) and CBS et al. (2015) (see section §3.1).

4.2 Model scenario study

4.2.1 Effects of slope

Orientation of slope had strong effects on drought stress for plants, with South slope having much higher stress than flat and North slope (Figure 13). This was because potential transpiration was much higher on South slope (on average 44.9 for South, 32.3 for flat, and 25.8 cm/year for North slope), whereas actual transpiration remained only slightly different (on average 32.1 for South, 25.3 for flat, and 19.1 cm/year for North slope) due to lack of available soil water.

Due to the stronger drought stress, plant biomass was slightly lower on South slope. The effect on biomass, however, was not so prominent, because plant production in summer was also strongly limited by nutrient availability in soil. Difference in soil C accumulation rates among slopes was even smaller, because less plant production in South slope (and therefore less litter input to soil) was compensated by lower SOM decomposition rates on South slope due to drought stress.

The model predicted a different probability of associations on North and South slope than on flat surface (Figure 14 for lime-poor dunes; Figure 15 for lime-rich dunes. In lime-poor dunes, 14AA02 *Violo-Corynephoretum* and 14CA01 *Phleo-Tortuletum ruraliformis (*in the early stages of succession only) is predicted to occur more on the South slope than flat and North slope, at the expense of 14BB02 *Festuco-Galietum veri*, 14CB01 *Taraxaco-Galietum veri*, and 20AB02 (*Polypodio-Empetretum*) (Figure 14). In lime-rich dunes, the effect of slope was less prominent: 14CA01 *Phleo-Tortuletum ruraliformis* occurred more often at the South slope compared to the flat surface, while 14CB01 *Taraxaco-Galietum veri* and 14AA02 *Violo-Corynephoretum* occurred less at the South slope.

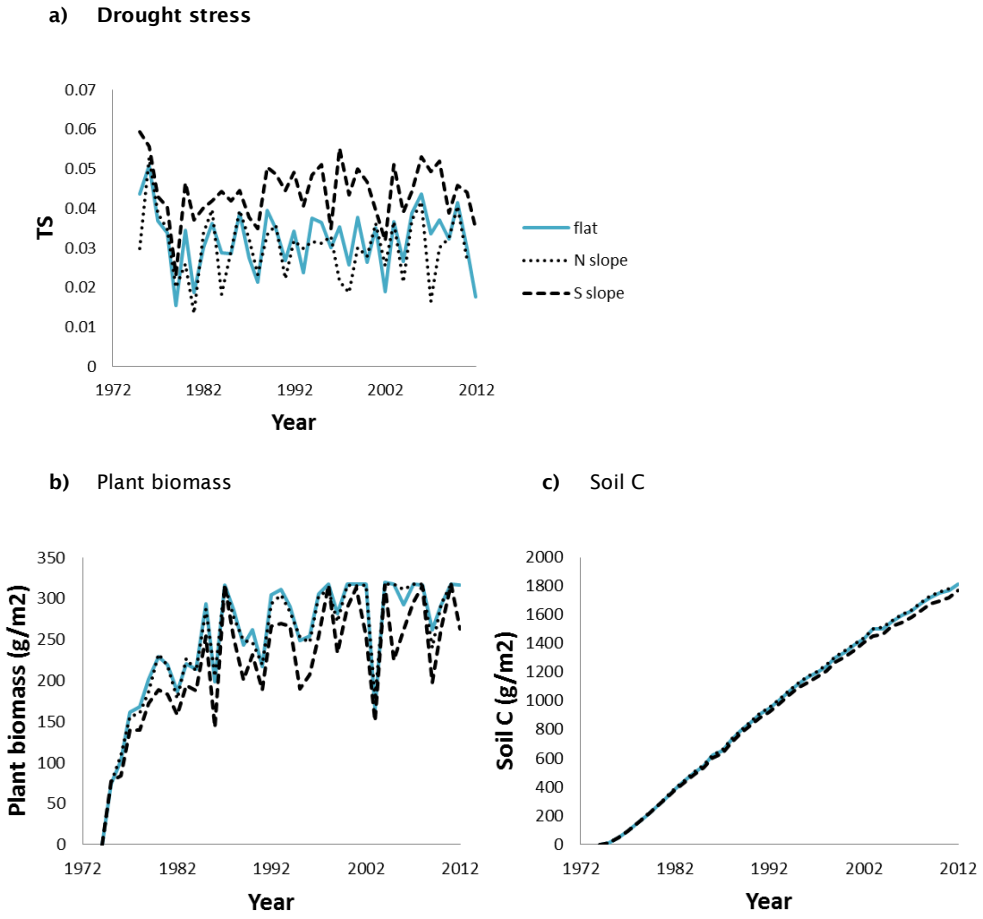

Figure 13. Drought stress (a), above-ground vascular plant biomass (b), and soil C accumulation (C) for 38 years model simulation of dune grasslands in Luchterduinen under three scenarios of slope: flat, South slope, and North slope.

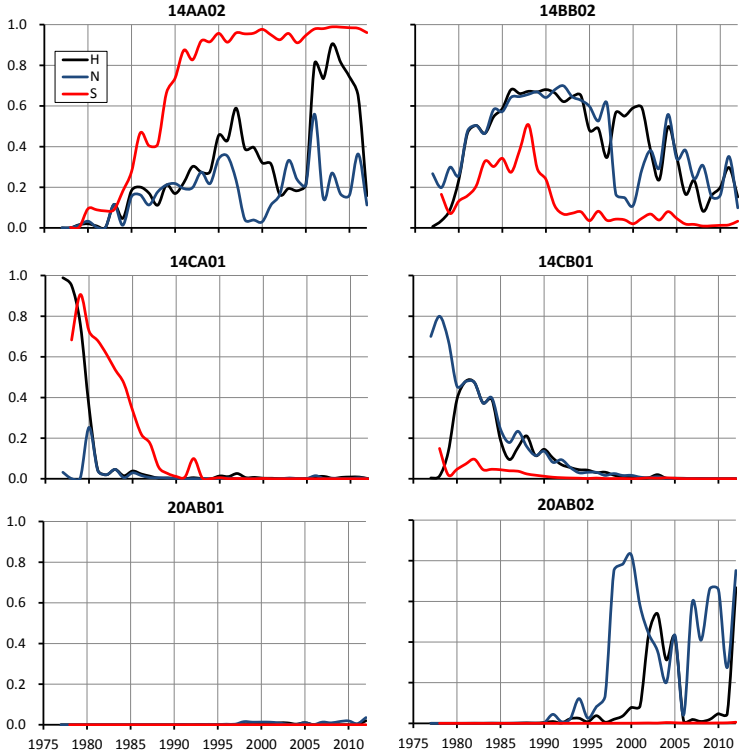

Figure 14. Vegetation development for 38 years on a lime-poor dune soil with a horizontal surface (H), a south-slope (S) and a north-slope (N).

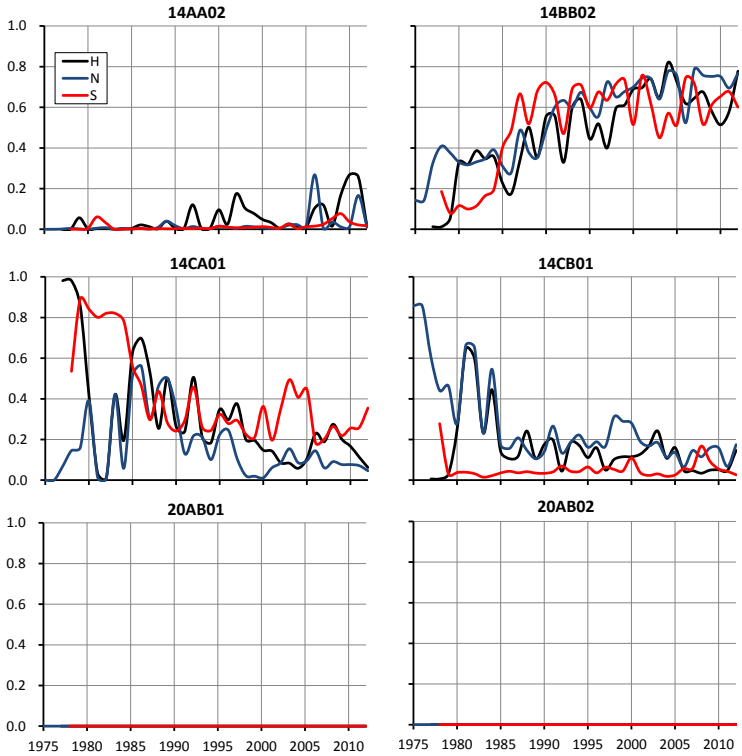

Figure 15. Vegetation development for 38 years on a lime-rich dune soil with a horizontal surface (H), a south-slope (S) and a north-slope (N).

4.2.2 Effects of future climate

The model predicted that climate change hardly affect soil organic matter accumulation rate of dunes starting from bare soil (Figure 16a). Plant biomass showed a slight decrease for the future climatic conditions relative to the current conditions (Figure 16b). Plant growth was suppressed due to increased drought stress under the future climate conditions, yet it was largely compensated by positive effects of higher future air temperature on plant growth. The N-leaching to the deeper groundwater hardly changed under the future climate conditions (Figure 16d).

For model simulations starting from old grassland, soil organic matter accumulation rate decreased slightly under the future climate conditions (Figure 17b). This was mainly due to decreased plant biomass (Figure 17b). The effects of future climate on groundwater recharge and N leaching was not consistent among years and not very significant (Figure 17 c&d).

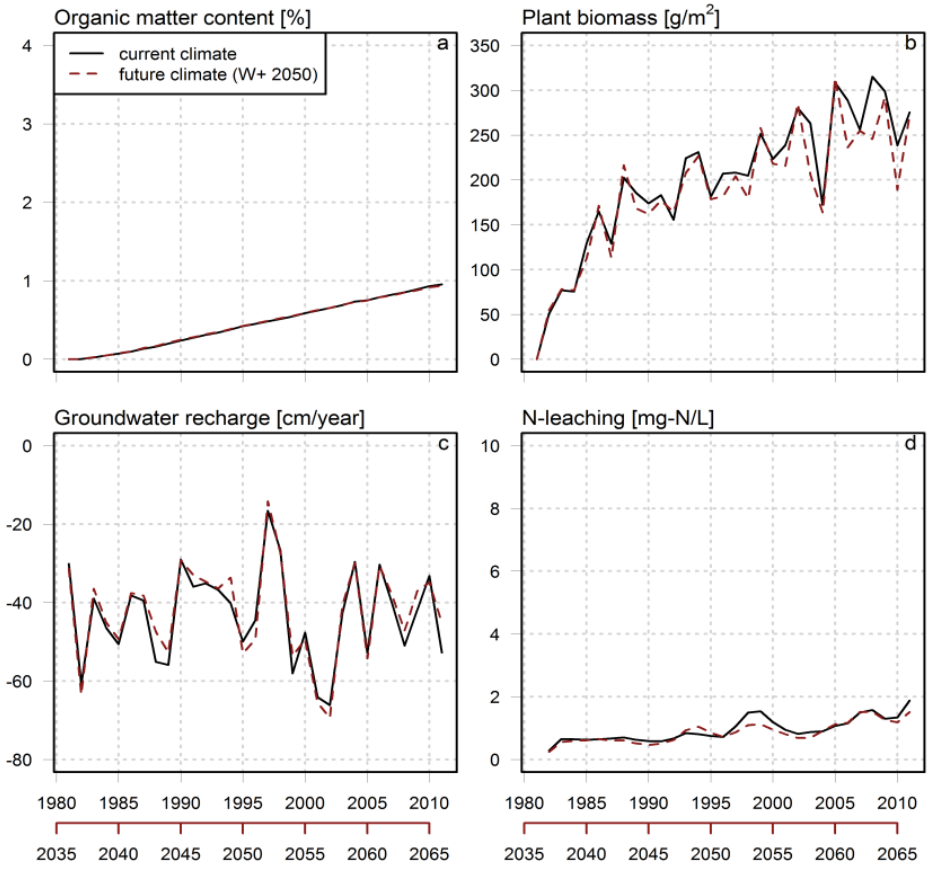

Figure 16: Organic matter content (a), above-ground vascular plant biomass (b), groundwater recharge (c) and N-leaching (d) for 30 years model simulation of dune grasslands in Luchterduinen under two climate scenarios: current climate (1981-2010) and KNMI'06 climate scenario W+ for 2050. Initial soil cover for these simulations is bare soil.

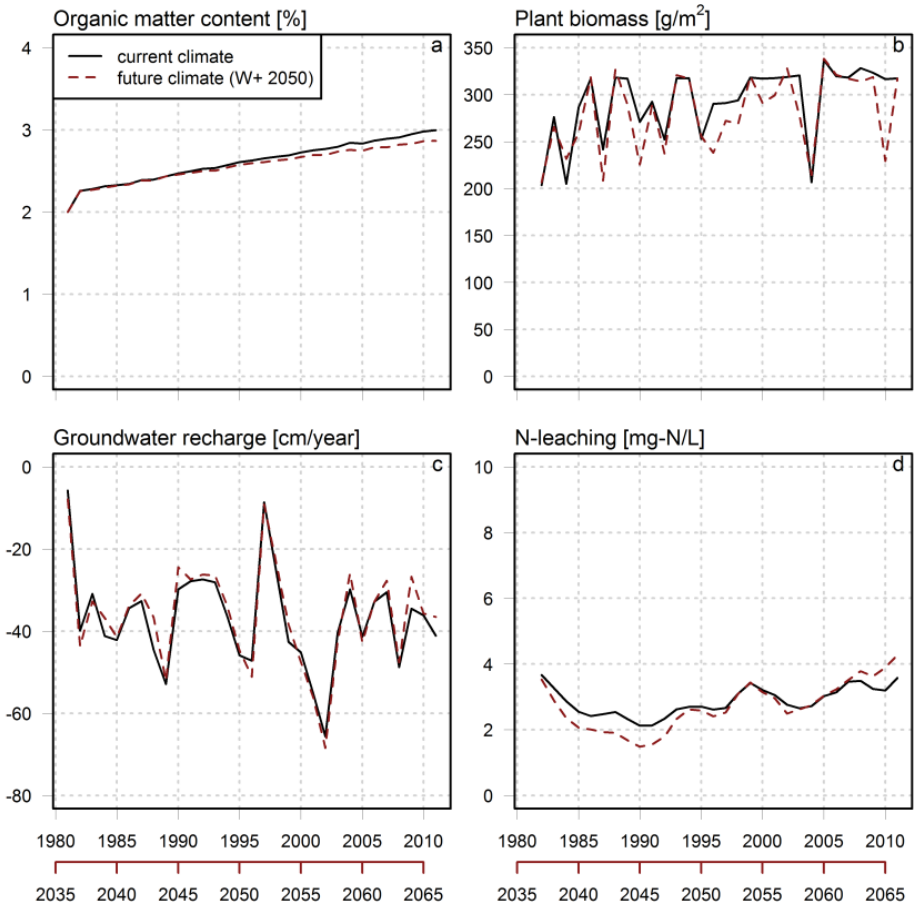

Figure 17: Organic matter content (a), above-ground vascular plant biomass (b), groundwater recharge (c) and N-leaching (d) for 30 years model simulation of dune grasslands in Luchterduinen under two climate scenarios: current climate (1981-2010) and KNMI'06 climate scenario W+ for 2050. Initial soil cover for these simulations is old grassland.

Our model predicted that future climate changes habitat conditions for plants. Under future climate, drought stress would increase (Figure 18 left) and N mineralization rate would slightly increase (Figure 18 right), whereas soil pH would be hardly influenced. Consequently, future climate would also influence the dominant vegetation types (Figure 19). Under future climate, in lime-poor dunes, 14AA02 *Violo-Corynephoretum* and 14CA01 *Phleo-Tortuletum ruraliformis* increased and 14BB02 *Festuco-Galietum veri* decreased in the intermediate and late successional stages. In lime-rich dunes, different patterns were predicted: 14BB02 *Festuco-Galietum veri* increased whereas 14CA01 *Phleo-Tortuletum ruraliformis* decreased under future climate.

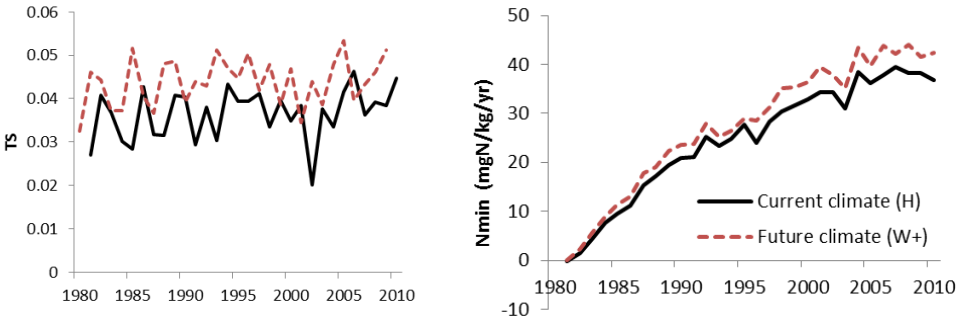

Figure 18. Predicted drought stress (left) and N mineralization (right) under two climate scenarios (H and W+) for 30 years model simulation of dune grasslands starting from a bare sand.

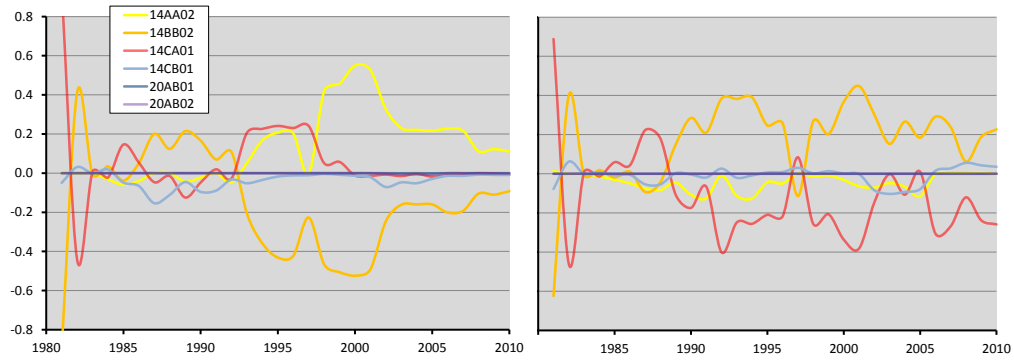

Figure 19. The effect of climate change scenario W+ on the development of the most dominant vegetation types on: (left) a lime-poor dune soil, and (right) on a lime-rich dune soil. The y-axis shows the change in simulates occurrence probability (positive values indicate an increase in the probability due to climate change, negative values a decrease).

4.2.3 Effects of nitrogen input via atmospheric deposition (Luchterduinen)

Lowering N deposition to the 1900 level decreased plant biomass production (Figure 20a) and N leaching (Figure 20b) during 30 years of dune succession starting from bare soils (which mimics the effects on early stage succession). The similar results were obtained when the simulation was started from old grasslands (which mimics the effects on late stage succession); lowering N deposition decreased plant production (Figure 20c) as well as N leaching (Figure 20d).

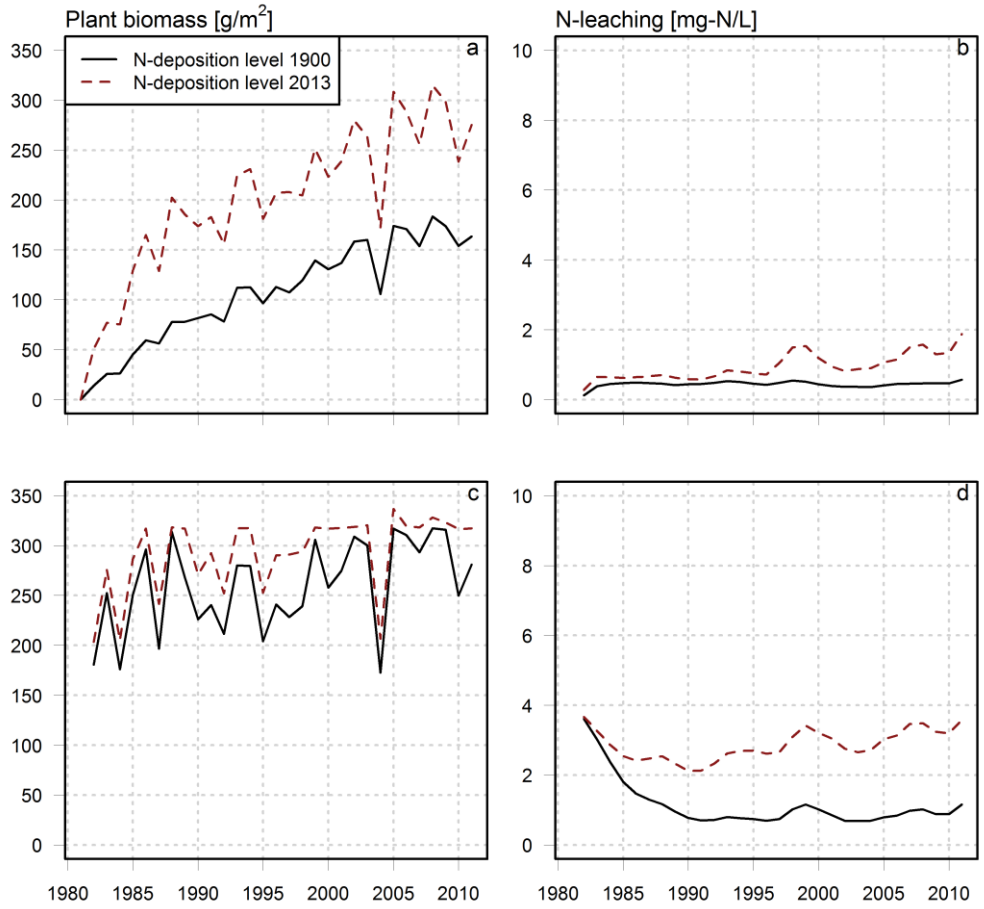

Figure 20: Above-ground vascular plant biomass (a,c) and N-leaching (b,d) for 30 years model simulation of dune grasslands in Luchterduinen under two scenarios of atmospheric N deposition: 1900 level and 2013 level. Initial soil cover for these simulations is bare soil (top) or old grasslands (bottom).

4.2.4 Effects of nitrogen input via manure (production grassland in Limburg)

Our model predicted that increasing N manure elevated the level of N leaching (Figure 21). This was because the plant biomass production becomes not limited by nitrogen when N manure level goes above 16gN/m^2/year, and therefore the excess of nitrogen in soil is not taken up by plants but leaches into groundwater. When the N manure level is high (32 gN/m^2/year), the N concentration in the leachate was predicted to exceed the level of the Dutch drinking water norm, 50 mgNO_3/L.

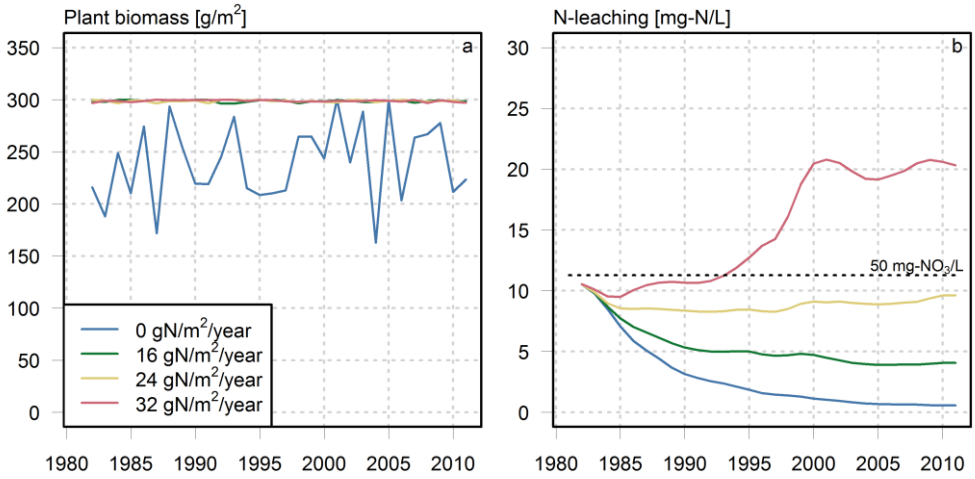

Figure 21: Above-ground vascular plant biomass (a) and N-leaching (b) for 30 years models simulation of agricultural grasslands in Limburg on a loess soil under four manure scenarios.

5 Discussion

5.1 Consequences of dynamic coupling of CENTURY and SWAP models

One of the major consequences of the dynamic coupling between the CENTURY and SWAP models is the update of soil physical characteristics based on SOM accumulation. However, even for the longest simulation period (i.e. 75 years) of dune grasslands, the accumulation of SOM in this poorly productive ecosystem reaches approximately 2%. The small changes in SOM led to a slight shift in the water retention curve (Figure 22).

The relatively small changes in water retention curves in our modelling exercise were also because of our choice on the repro-function of Wösten *et al.* (2001). This reprofunction has an advantage that it covers all types of soil types, whereas it used limited amount of soil samples for each soil type and therefore the reliability of the estimated parameter values for our dune ecosystem are questionable. For sandy soils, we derived repro-functions based on more extensive soil data set of dune grasslands in Meijendel (Fujita & Aggenbach, 2015). The estimated parameter values are largely different between two studies, and so is the water retention curve (Figure 23). Thus, not surprisingly, the choice of the reprofunction will have a large consequence on how soil development influences soil physical characteristics in the model.

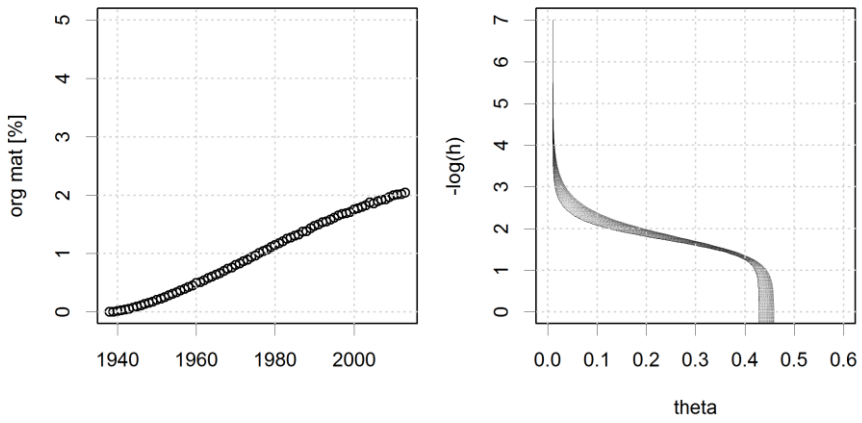

Figure 22. Change in soil organic matter content (left) and soil water retention curve (volumetric water content (cm^3/cm^3) versus logarithm of pressure head (cm), right) during 75 years simulation period in Lucthterduinen. The soil water retention curve was written 75 times for each simulation year.

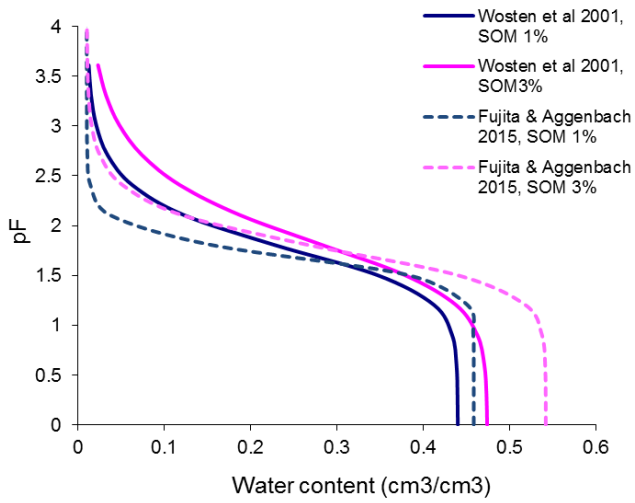

Figure 23. Comparison of water retention curves of sandy soils between those based on repro-function of Wösten et al. 2001 (solid lines) and those based on Fujita & Aggenbach 2015 (dashed lines). Water retention curves were drawn for 1% and 3% of soil organic matter content. For the repro-function of Wösten, we assumed silt plus clay content as 5%, grain size as 200 µm.

Another consequence of the dynamic coupling of SWAP and CENTURY is the yearly update of soil cover in SWAP. By explicitly modelling the increase in soil cover in the course of dune succession, the model can reproduce the pattern that soil evaporation is relatively high and transpiration is low in the early stage of succession (Figure 24). It should be noted that our model does not explicity consider mosses and lichens, whereas they could have prominent influence on evaporation (Voortman *et al.*, 2013b), especially in early stages of dune succession in which vascular plant cover is still sparse. Thus, in order to more realistically simulate water balance in dunes, it is necessary to incorporate mosses and lichen vegetation in the hydrological model.

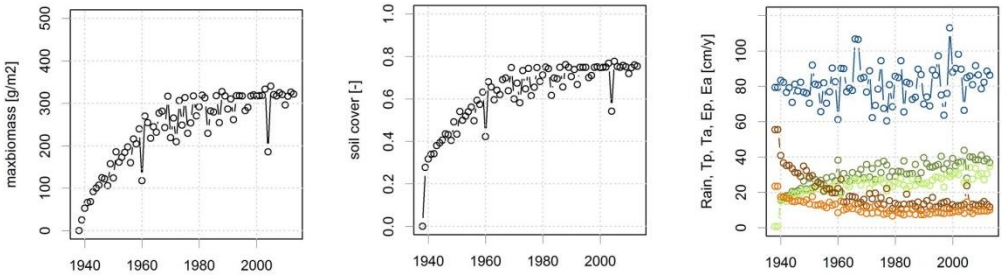

Figure 24. Change in vascular plant biomass at the peak growing season (left), soil cover (middle) and water balance (right) during the 75-year simulation of dune succession. In the right figure, blue points represent rain (cm/yaer); brown and orange points represent potential and actual evaporation (cm/year), respectively; dark green and light green points represent potential and actual transpiration (cm/year), respectively.

5.2 Plausibility and uncertainty of the models

Our model could reproduce soil development of dune succession well. For the succession of up to 75 years, the model predicted the rate of soil C and N accumulation in the same range to those observed in the field in Luchterduinen.

In terms of plant biomass, the predicted values by our model were higher than the observed values in the field. This mismatch can be explained by several missing processes. Grazing

animals (e.g. rabbits) were common in this area, yet our CENTURY model does not include grazing processes (i.e. removal of above- and below-ground plant biomass by animals, addition of urine and feces). More adequate field sampling of biomass (e.g. biomass in enclosure to exclude the effect of grazers) will help testing the model prediction for plant production. Furthermore, biomass production of mosses can be sometimes higher than that of vascular plants in dune ecosystems, whereas CENTURY model only include vascular plants. Explicit inclusion of these processes, together with proper estimation of input and parameter values regarding these processes, would improve our model prediction.

The shift in vegetation types during dune succession was predicted reasonably well. The predicted differences in dominant vegetation types between lime-poor and lime-rich dunes and between early and later successional stages were largely in accordance with field observations and Schaminée and Jansen (1998). The prediction was poorest for the vegetation types 14BB02 *Festuco-Galietum veri* and 14CB01 *Taraxaco-Galietum veri*, the two vegetation types which are associated with relatively high nutrient indicator values. Although the combined prediction of these two vegetation types matches reasonably well with the observation, division between them were not right. Furthermore, the model predictions for the two heath vegetations (20AB01 and 20AB01) were not entirely correct: the commonly observed heath 20AB01 (*Carici arenariae-Empetretum)* was only marginally predicted, whereas the presence of the other heath 20AB02 (*Polypodio-Empetretum)* was overestimated especially on flat surface. These poor predictions may be caused by the uncertainty in the empirically-derived relationship between nutrient availability and indicator values of plants for nutrients. Because the increase in nutrient availability during dune succession is not drastic, we need a better repro-function that can reflect subtle changes in nutrient availability on vegetation types. To improve the repro-function, more extensive dataset of the target ecosystems is inevitable.

Another factor which challenges the prediction of vegetation types is the time-lag in plant response. In the model, when an environmental condition changes, the vegetation type which adapts the best to the new condition is always selected, irrespective of the preceding vegetation types. In reality, however, plants do not respond to environmental changes immediately, because existing plants can, at least to some extent, persist by plastically responding to the changed conditions, and also because new species which is potentially most adapted to the new habitat conditions must arrive at the place before they establish. In this study, we used 4-year average of indicator values to reflect the time-lag of plant response. In order to tackle this problem more properly, the model needs to be extended to include dispersal processes and delayed response of plants. To this end we should define the response time of vegetation types on the basis of their observed spectrum of plant functional types such as annuals (quick response), biennials, perrenials and geophytes (slow response).

Our CENTURY model was validated for natural dune ecosystems, but not for agricultural lands in Limburg due to lack of empirical dataset. This leads to a large uncertainty of our model prediction for the Limburg site. To make the model more robust for the agricultural lands, our CENTURY model needs the following modifications. First, parameter values for plant production and shoot:root ratio should be calibrated with suitable field observation data. These parameters are sensitive to, among others, SOM accumulation rates and N leaching rates. Second, the manuring should be better mimicked in the model. In Limburg, manure is usually applied by injecting organic manure in top soil, whereas in our model manure was applied in a form of mineral N. To properly trace the effects of manure in the soil, the application method of manure should be more properly incorporated in the CENTURY model.

5.3 Effects of slope and climate change

Our model predicted that orientation of slope influences drought stress for plants and therefore vegetation types. Although our field records are not enough to quantitatively validate the model predictions on different slopes, we could evaluate the plausibility based on expert knowledge (per.comm. Martin de Haan (KWR)). For example, 14AA02 *Violo-Corynephoretum*, the vegetation type which was predicted to occur much more at South slopes than flat of North slopes, occur commonly on S slopes (but also on flat surface) in the field. 20AB02 *Polypodio-Empetretumi* is often observed on N slope in the field, and model also predicted that this vegetation type occurs more often on N slope than on flat surface. Furthermore, the model also predicted that orientation of slope has only minor impacts on plant production (i.e. less biomass on South slope) and little effects on SOM accumulation. This is not in line with the patterns observed in the field that South slopes are usually associated with less biomass and poor SOM development.

Note that our model is not (yet) able to capture the effect of slopes on soil temperature. Therefore, the predicted patterns in vegetation and soil on different slopes were primarily caused by the difference in soil moisture only. This means that the real effects of slope could be larger than what we predicted in this study, supposing a strong impact of heat stress on plants and soil microorganisms.

Our model predicted that effects of future climate on SOM accumulation and plant production would be minor. However, there are several uncertain factors which could have large impacts on the predictions. SOM accumulation and plant production are very sensitive to the parameter values of the temperature-dependent terms in soil decomposition and plant growth. The temperature sensitivity of soil decomposition (so called Q10 values) are known to depend on multiple factors such as chemical and physical properties of soil carbon (e.g. Fiere et al. 2006, Davidson et al. 2006), while these factors varies largely among locations and development stages. Due to the uncertainties, there is still no consensus among scientific communities whether soils become sink or source of CO_2 under warming (Davidson & Janssens, 2006; Kirschbaum, 2006; Conant *et al.*, 2011).

Although the predicted effects of future climate on SOM and plant production were small, future climate could have a substantial impact on habitat factors for plants and therefore influence vegetation types. The model predicted that drought stress and nutrient availability increase under climate change. Note that difference in preferred nutrient availability levels among the six vegetation types were very small. This means that a small error in either prediction of nutrient availability or the reprofunction of nutrient availability versus indicator value can result in very different prediction of vegetation types. The unexpected predictions of climate change (e.g. opposite pattern of vegetation types under future climate between lime-rich and lime-poor dunes) may be just an artefact of such uncertainty in the model prediction.

5.4 Effects of N input on N leaching

Our model predicted that reducing atmospheric N deposition decreased plant production and N leaching, both for the simulation starting from a bare soil (i.e. early successional stage) and from an old grassland (i.e. late successional stage). The impacts of reduced N deposition on N leaching were stronger for late than early stage of succession. This is because a large part of N input via atmospheric deposition is taken up by plants in SOM-poor early stage, whereas in SOM-rich late stage N input via atmospheric deposition is not taken up by plants but leaches out. This indicates that reduction of N deposition has a greater potential to lower N leaching especially in old dune grasslands. Note that another study of Luchterduinen showed a contradictory pattern that elevated atmospheric N deposition does

not increase soil N accumulation and plant production, presumably due to the dominant effects of biological N fixation (Aggenbach *et al*., Submitted). Therefore, we still need better understanding on the effects of N input on soil development and N cycles before drawing a conclusion on their consequence in N leaching rates.

The model predicted that manure application to agricultural lands leads to increased N leaching. As soon as the amount of N manure reaches the level in which plant production is not limited by nitrogen anymore, increased N manure results in drastic increase in N leaching.

Due to lack of empirical data, we were not able to quantitatively validate our model results of N leaching. To assess the model plausibility in predicting N leaching, field measurements of leachates are needed. Since a number of processes influence N leaching, monitoring of N leaching rates should be combined with measurements of other relevant process rates such as evapotranspiration, atmospheric N deposition rates, SOM decomposition rates, plant growth, etc. Lysimeters with a controlled lower boundary (soil suction plate) to mimic field conditions are excellent devices to investigate these processes.

6 Conclusions and recommendations

In this study we developed a new version of PROBE model (PROBE-3), which, for the first time, dynamically couples the models of hydrology, soil, plant production, and vegetation types to predict ecosystem services (i.e. vegetation types, N leaching, groundwater recharge). The dynamic coupling enabled to explicitly simulate changes in soil physical characteristics and changes in evapotranspiration in the course of dune succession. These features of the model are important to adequately evaluate the effects of climate change, because the feedback between water, soil, and plant could amplify or mitigate the climate effects on a long term.

Our extensive field observation data in natural dune ecosystems enabled to evaluate the plausibility of the PROBE-3. Overall, soil development (in terms of carbon and nitrogen accumulation) and vegetation types during 75-year dune succession were predicted well or quite well by the model depending on the vegetation type. Plant production and N leaching were predicted in the same range to field observation, but better field data is needed to verify the model performance for these variables.

The model scenario studies indicated that slope has a minor influence on soil organic matter accumulation and plant production, but a prominent effect of vegetation types. Similarly, the model predicted that future climate leads to little impacts on soil organic matter accumulation, plant production, groundwater recharge and N leaching, but a significant effect on vegetation types. Increased atmospheric N deposition in dune ecosystems and increased N manure in agricultural land are both expected to increase N leaching rates,

We identified several uncertainties in the model. To further improve the model, we need more empirical data for model validation (e.g. N leaching in natural and agricultural lands, plant production) and for better reprofunctions (e,g, nutrient availability versus indicator value of plants, parameter values of water retention curves versus soil organic matter content). Furthermore, several important processes should be added to the model to make the long-term prediction of future climate changes more robust. That includes delayed responses of plant species to environmental changes, impacts of mosses on soil physical characteristics and on nutrient cycle, and substrate-specific temperature dependency of SOM decomposition.

References

Aarts, H.F.M., Daatselaar, C.H.G. & Holshof, G. (2005) Bemesting en opbrengst van productiegrasland in Nederland. In, p. 34

Aggenbach, C., Kooijman, A., Fujita, Y., Van Der Hagen, H., Van Til, M., Cooper, D. & Jones, M.L.M. (Submitted) Does atmospheric nitrogen deposition lead to greater nitrogen and carbon accumulation in coastal sand dunes?

Aggenbach, C.J.S., Kooijman, A.M., Bartholomeus, R.P. & Fujita, Y. (2013) Herstelbaarheid van droge duingraslanden in relatie tot accumulatie van organische stof en stikstof in de bodem. In, p. 73. KWR Watercycle Research Institute

Bartholomeus, R.P., Witte, J.P.M. & Cirkel, D.G. (2010) Climate change effects on vegetation characteristics and groundwater recharge. Poster presentation. *EGU General Assembly 2010* (ed by. Vienna, Austria.

Bartholomeus, R.P., Witte, J.P.M. & Runhaar, J. (2011a) Drought stress and vegetation characteristics on sites with different slopes and orientations. *Ecohydrology*, **5**, 808-818.

Bartholomeus, R.P., Voortman, B. & Witte, J.P.M. (2013) Metingen en proceskennis vereist voor betrouwbare verdampingsberekening in grondwatermodellen. *Stromingen*, **19**

Bartholomeus, R.P., Witte, J.P.M., Van Bodegom, P.M., Van Dam, J.C. & Aerts, R. (2011b) Climate change threatens endangered plant species by stronger and interacting water-related stresses. *J. Geophys. Res.*, **116**, G04023.

Bennie, J., Huntley, B., Wiltshire, A., Hill, M.O. & Baxter, R. (2008) Slope, aspect and climate: Spatially explicit and implicit models of topographic microclimate in chalk grassland. *Ecological Modelling*, **216**, 47-59.

Bindi, M., Miglietta, F. & Zipoli, G. (1992) Different methods for separating diffuse and direct components of solar radiation and their application in crop growth models. *Climate Research*, **2**, 47-54.

CBS, PBL & Wageningen UR (2015) *Verzurende depositie, 1981-2013 (indicator 0184, versie 14, 5 januari 2015). www.compendiumvoordeleefomgeving.nl*. Available at: www.compendiumvoordeleefomgeving.nl (accessed 20150820 2015).

Cleveland, C.C. & Liptzin, D. (2007) C:N:P stoichiometry in soil: Is there a "Redfield ratio" for the microbial biomass? *Biogeochemistry*, **85**, 235-252.

Conant, R.T., Ryan, M.G., Agren, G.I., Birge, H.E., Davidson, E.A., Eliasson, P.E., Evans, S.E., Frey, S.D., Giardina, C.P., Hopkins, F.M., Hyvonen, R., Kirschbaum, M.U.F., Lavallee, J.M., Leifeld, J., Parton, W.J., Megan Steinweg, J., Wallenstein, M.D., Martin Wetterstedt, J.A. & Bradford, M.A. (2011) Temperature and soil organic matter decomposition rates - synthesis of current knowledge and a way forward. *Global Change Biology*, **17**, 3392-3404.

Davidson, E.A. & Janssens, I.A. (2006) Temperature sensitivity of soil carbon decomposition and feedbacks to climate change. *Nature*, **440**, 165-173.

De Haan, M.W.A. & Doomen, A. (2006) Optimalisatie natuur en waterwinning in de Amsterdamse Waterleidingduinen. Milieueffectrapport - deelrapport natuur en landschap. In. Kiwa Water Research, Nieuwegein.

De Haan, M.W.A. & Witte, J.P.M. (2010) Onderdeel effectbeschrijving met behulp van PROBE van de Milieu Effect Rapportage Optimalisatie Bedrijfsvoering Noord Hollands Duinreservaat. In. NV PWN Waterleidingbedrijf Noord-Holland, Velserbroek.

De Lima, J.L.M.P. (1990) The effect of oblique rain on inclined surfaces: a nomograph for the rain-gauge correction factor. *Journal of Hydrology*, **115**, 407-412.

De Wit, C.T. (1958) *Transpiration and crop yields*. Pudoc, Wageningen.

Dyer, J. (2009) Assessing topographic patterns in moisture use and stress using a water balance approach. *Landscape Ecology*, **24**, 391-403.

Easterling, D.R., Meehl, G.A., Parmesan, C., Changnon, S.A., Karl, T.R. & Mearns, L.O. (2000) Climate extremes: observations, modeling, and impacts. *Science*, **289**, 2068-2074.

Fay, P.A., Kaufman, D.M., Nippert, J.B., Carlisle, J.D. & Harper, C.W. (2008) Changes in grassland ecosystem function due to extreme rainfall events: implications for responses to climate change. *Glob. Change Biol.*, **14**, 1600-1608.

Fujita, Y. & Aggenbach, C.J.S. (2015) Patterns of soil development and plant species diversity in Grey Dunes in Meijendel. In. KWR Watercycle Research Institute

Fujita, Y., van Bodegom, P.M. & Witte, J.-P.M. (2013a) Relationships between Nutrient-Related Plant Traits and Combinations of Soil N and P Fertility Measures. *PLoS ONE*, **8**, e83735.

Fujita, Y., van Bodegom, P.M., Olde Venterink, H., Runhaar, H. & Witte, J.-P.M. (2013b) Towards a proper integration of hydrology in predicting soil nitrogen mineralization rates along natural moisture gradients. *Soil Biology and Biochemistry*, **58**, 302-312.

Kirschbaum, M.U.F. (2006) The temperature dependence of organic-matter decomposition - Still a topic of debate. *Soil Biology and Biochemistry*, **38**, 2510-2518.

Knapp, A.K., Beier, C., Briske, D.D., Classen, A.T., Luo, Y., Reichstein, M., Smith, M.D., Smith, S.D., Bell, J.E., Fay, P.A., Heisler, J.L., Leavitt, S.W., Sherry, R., Smith, B. & Weng, E. (2008) Consequences of more extreme precipitation regimes for terrestrial ecosystems. *BioScience*, **58**, 811-821.

Kooijman, A.M., Bloem, J., Cerli, C., Jagers Op Akkerhuis, G.A.J.M., Kalbitz, K., Dimmers, W.J., Vos, A., Peest, A.K. & Kemmers, R.H. (2014) Stikstofkringloop in kalkrijke en kalkarme duinbodems : en de implicaties daarvan voor de effectiviteit van plaggen. In. Vereniging van Bos- en Natuureigenaren, Driebergen.

Kruijt, B., Witte, J.P.M., Jacobs, C.M.J. & Kroon, T. (2008) Effects of rising atmospheric CO2 on evapotranspiration and soil moisture: A practical approach for the Netherlands. *Journal of Hydrology*, **349**, 257-267.

Levine, J.M., McEachern, A.K. & Cowan, C. (2008) Rainfall effects on rare annual plants. *J. Ecol.*, **96**, 795-806.

Makkink, G.F. (1957) Testing the Penman formula by means of lysimeters. *Journal of the Institution of Water Engineers*, **11**, 277-288.

Manzoni, S., Schimel, J.P. & Porporato, A. (2011) Responses of soil microbial communities to water-stress: Results from a meta-analysis. *Ecology*, **93**, 930-938.

Mentens, J., Raes, D. & Hermy, M. (2003) Effect of orientation on the water balance of greenroofs. *Greening Rooftops for Sustainable Communities* (ed by, pp. 363-371. Chicago.

Metherell, A.K., Harding, L.A., Cole, C.V. & Parton, W.J. (1993) *CENTURY soil organic matter model environment. Technical documentation agroecosystem version 4.0.*

Noordijk, H. (2007) Nitrogen in the Netherlands over the past fivecenturies. *First International Ammonia Conference in Agriculture* (ed by G.J. Monteny and E. Hartung). Ede, Nederland.

Parton, W.J., Schimel, D.S., Cole, C.V. & Ojima, D.S. (1987) Analysis of Factors Controlling Soil Organic-Matter Levels in Great-Plains Grasslands. *Soil Science Society of America Journal*, **51**, 1173-1179.

Parton, W.J., Scurlock, J.M.O., Ojima, D., Gilmanov, T.G., Scholes, R.J., Schimel, D.S., Kirchner, T., Menaut, J.-C., Seastedt, T., Garcia Moya, E., Kamnalrut, A. & Kinyamario, J.I. (1993) Observations and modeling of biomass and soil organic matter dynamics for the grassland biome worldwide. *Global Biogeochemical Cycles*, **7**, 785-809.

Porporato, A., Daly, E. & Rodriguez-Iturbe, I. (2004) Soil water balance and ecosystem response to climate change. *Am. Nat.*, **164**, 625-632.

Reed, S.C., Cleveland, C.C. & Townsend, A.R. (2011) Functional Ecology of Free-Living Nitrogen Fixation: A Contemporary Perspective. *Annual Review of Ecology, Evolution, and Systematics*, **42**, 489-512.

Schaminée, J.H.J. & Jansen, A.J.M. (1998) Wegen naar natuurdoeltypen; ontwikkelingsreeksen en hun indicatoren ten behoeve van herstelbeheer en natuurontwikkeling (sporen A en B). In. Wageningen, IKC Natuurbeheer, 1998. Rapport 26, 320 blz

Schaminée, J.H.J., Weeda, E.J. & Westhoff, V. (1995) *De vegetatie van Nederland. Wateren, moerassen, natte heiden.* Opulus Press, Uppsala, SE, Leiden, NL.

Schaminée, J.H.J., Stortelder, W. & Weeda, E.J. (1996) *De vegetatie van Nederland. Graslanden, zomen, droge heiden.* Opulus Press, Uppsala, SE, Leiden, NL.

Schaminée, J.H.J., Weeda, E.J. & Westhoff, V. (1998) *De vegetatie van Nederland.* Opulus Press, Uppsala, SE, Leiden, NL.

Schmidt, J. & Mauersberger, F. (2009) Wind effects on soil erosion by water. *Advances in GeoEcology* (ed. by A. Faz Cano, A.R. Mermut, J.M. Arocena and R. Ortiz), pp. 201-206. Catena Verlag, Reiskirchen.

Stiboka (1990) Bodemkaart van Nederland schaal 1 : 50 000. Toelichting bij de kaartblad 61 - 62 West en Oost Maastricht - Heerlen. Stichting voor Bodemkartering, Wageningen.

Stortelder, A.H.F., Schaminée, J.H.J. & Hommel, P.W.F.M. (1999) *De vegetatie van Nederland*. Opulus Press, Uppsala, SE, Leiden, NL.

Stuyfzand, P.J. (1991) Samenstelling, genese en kwaliteitsvariaties van ondiep grondwater in kustduinen. In, p. 175

Stuyfzand, P.J. (2010) Modellering kwaliteit ondiep (duin)grondwater en ontkalking, inclusief effecten van atmosferische depositie, klimaatverandering en kustuitbreiding: DUVELCHEM. In:

Stuyfzand, P.J. & Rambags, F. (2011) Hydrologie en hydrochemie van de 4 lysimeters te Castricum; Overzicht van resultaten met uitzicht op haalbaarheid van reanimatie van het lysimeterstation. In. KWR

Šúri, M. & Hofierka, J. (2004) A new GIS-based solar radiation model and its application to photovoltaic assessments. *Transactions in GIS*, **8**, 175-190.

Van Dam, J.C., Groenendijk, P., Hendriks, R.F.A. & Kroes, J.G. (2008) Advances of modeling water flow in variably saturated soils with SWAP. *Vadose Zone Journal*, **7**, 640-653.

Van der Knaap, Y., Bakker, M.M., Alam, S.J., Witte, J.P.M., Van Ek, R., Bierkens, M.F.P. & Van Bodegom, P.M. (submitted) Land use changes determine vegetation patterning more than climate change or climate adaptation measures. *Land Use Policy*,

Van der Knaap, Y.A.M., De Graaf, M., van Ek, R., Witte, J.-P.M., Aerts, R., Bierkens, M.F.P. & Van Bodegom, P.M. (2015) Potential impacts of groundwater conservation measures on catchment-wide vegetation patterns in a future climate. *Landscape Ecology*, **30**, 855-869.

Van Ek, R., Witte, J.P.M., Mol-Dijkstra, J.P., De Vries, W., Wamelink, G.W.W., Hunink, J., Van der Linden, W., Runhaar, J., Bonten, L., Bartholomeus, R., Mulder, H.M. & Fujita, Y. (2014) Ontwikkeling van een gemeenschappelijke effect module voor terrestrische natuur. In, p. 150. STOWA, Amersfoort.

Velders, G.J.M., Aben, J.M.M., Geilenkirchen, G.P., den Hollander, H.A., Noordijk, E., van der Swaluw, E., de Vries, W.J., Wesseling, J. & van Zanten, M.C. (2015) Grootschalige concentratie- en depositiekaarten luchtverontreiniging. In. RIVM, Bilthoven.

Voortman, B., Witte, J.P.M., Van Rheenen, H., Bosveld, F., Elbers, J., Van der Bolt, F., Heijkers, J., Hoogendoorn, J., Bolman, A., Spek, T. & Voogt, M. (in prep) Resultaten van een nieuwe en handzame lysimeter; eerste stap naar een nationaal netwerk voor de werkelijke verdamping? *Stromingen*,

Voortman, B.R., Bartholomeus, R.P., Bosveld, F. & Witte, J.P.M. (submitted) Improving the performance of lysimeters with the aid of thermal imaging. *Journal of Hydrology*,

Voortman, B.R., Bartholomeus, R.P., van der Zee, S.E.A.T.M., Bierkens, M.F.P. & Witte, J.P.M. (2015) Quantifying energy and water fluxes in dry dune ecosystems of the Netherlands. *Hydrol. Earth Syst. Sci.*, **19**, 3787-3805.

Voortman, B.R., Bartholomeus, R.P., van Bodegom, P.M., Gooren, H., van der Zee, S.E.A.T.M. & Witte, J.-P.M. (2013a) Unsaturated hydraulic properties of xerophilous mosses: towards implementation of moss covered soils in hydrological models. *Hydrological Processes*, n/a-n/a.

Voortman, B.R., Bartholomeus, R.P., van Bodegom, P.M., Gooren, H., van der Zee, S.E.A.T.M. & Witte, J.-P.M. (2013b) Unsaturated hydraulic properties of xerophilous mosses: towards implementation of moss covered soils in hydrological models. *Hydrological Processes*, **28**, 6251-6264.

Weltzin, J.F., Loik, M.E., Schwinning, S., Williams, D.G., Fay, P.A., Haddad, B.M., Harte, J., Huxman, T.E., Knapp, A.K., Lin, G., Pockman, W.T., Shaw, M.R., Small, E.E., Smith, M.D., Smith, S.D., Tissue, D.T. & Zak, J.C. (2003) Assessing the response of terrestrial ecosystems to potential changes in precipitation. *BioScience*, **53**, 941-952.

Willems, W.J. & van Schijndel, M.W. (2012) Evaluatie Meststoffenwet 2012: syntheserapport. In. Planbureau voor de Leefomgeving, Den Haag.

Witte, J.-P.M., Bartholomeus, R.P., van Bodegom, P.M., Cirkel, D.G., van Ek, R., Fujita, Y., Janssen, G.M., Spek, T.J. & Runhaar, H. (2015a) A probabilistic eco-hydrological model to predict the effects of climate change on natural vegetation at a regional scale. *Landscape Ecology*, **30**, 835–854.

Witte, J., de Haan, M. & Hootsmans, M. (2007a) PROBE: een ruimtelijk model voor vegetatiedoelen. **24**, 77-87.

Witte, J.P.M., Kruijt, B., Kroon, T. & Maas, C. (2006) Verdamping planten daalt door toename atmosferische kooldioxyde. *H2O*, **5**, 29-31.

Witte, J.P.M., Wójcik, R.B., Torfs, P.J.J.F., De Haan, M.W.H. & Hennekens, S. (2007b) Bayesian classification of vegetation types with Gaussian mixture density fitting to indicator values. *J. Veg. Sci.*, **18**, 605-612.

Witte, J.P.M., Bartholomeus, R.P., Voortman, B., Van der Hagen, H. & Van der Zee, S.E.A.T.M. (2012a) Droge duinvegetatie zeer zuinig met water. *Landschap*, **3**, 109-117.

Witte, J.P.M., Bartholomeus, R.P., Dorland, E., De Haan, M. & Raterman, B. (2015b) PROBE voor de duinen van Dunea. In, p. 42. KWR Watercycle Research Institute, Niewegein.

Witte, J.P.M., Runhaar, J., van Ek, R., van der Hoek, D.C.J., Bartholomeus, R.P., Batelaan, O., van Bodegom, P.M., Wassen, M.J. & van der Zee, S.E.A.T.M. (2012b) An ecohydrological sketch of climate change impacts on water and natural ecosystems for the Netherlands: bridging the gap between science and society. *Hydrol. Earth Syst. Sci.*, **16**, 3945-3957.

Wösten, J.H.M., Veerman, G.J., de Groot, W.J.M. & Stolte, J. (2001) Waterretentie- en doorlatendheidskarakteristieken van boven- en ondergronden in Nederland: de Staringreeks. In: *Alterra-rapport*, p. 86. Alterra, Wageningen.